ABSTRACT

HATCH, TYLER R. Experimental Investigation into Plasma-Assisted Lean Prevaporized Non-Premixed Ignition. (Under the direction of Dr.Venkateswaran Narayanaswamy).

The current focus of the US military is to shift into one uniform fuel across all platforms. Heavy fuels represent a serious candidate for this due to their low flammability and ability to be stored for long periods. However, more experimentation is needed at real-life operating conditions for combustors. Turbulent flows of nonpremixed, lean fuel mixtures are common in many military applications. To investigate this, an apparatus for Jet-A fuel injection into a laser spark ignition system was developed. The fuel was prevaporized and mixed with heated nitrogen to obtain a lean fuel mixture for ignition experiments. The mixture was injected into a movable burner unit with air coflow to test the ignition probability of the mixture at different axial spark locations. Previous experiments with methane jets provided a baseline for the spark ignition experimentation with this setup. Experiments were conducted to obtain ignition probability maps, velocity profiles, and high-speed imaging of the spark system. Overall, three main factors influenced the results of this experiment: the temperature of the inlet flow, the phase of the fuel, and the fuel dilution rate in nitrogen. Future work will investigate ignition at higher temperatures and several spark locations upstream of the jet.

© Copyright 2018 Tyler R Hatch
All Rights Reserved

Experimental Investigation into Plasma-Assisted Lean Prevaporized Non-Premixed Ignition

by
Tyler R Hatch

A thesis submitted to the Graduate Faculty of
North Carolina State University
in partial fulfillment of the
requirements for the Degree of
Master of Science

Aerospace Engineering

Raleigh, North Carolina

2018

APPROVED BY:

_____	_____
Dr. Kevin Lyons	Dr. Kenneth Granlund

_____
Dr. Venkateswaran Narayanaswamy
Committee Chair

DEDICATION

For Juno.

BIOGRAPHY

Tyler Hatch was born in Wilmington, NC. He completed his B.S. in Aerospace Engineering at NC State in 2015 and will be working for NASA's Glenn Research Center in Cleveland, Ohio as a Research Aerospace Engineer in the Fluid Physics and Transport group upon completion of his Master's program.

ACKNOWLEDGEMENTS

I would like to thank the many people who made this project possible. Specifically: my labmates Vikram Ramnath, Kevin Ley, Aravind Ramachandran, Dominic Zelenak, Joshua Pickles, Sai Kiran Bavgi; other students from NC State who assisted me with this project including Tyler Farr, Eric Stewart, and Alex Hsain; students from the KAUST program including Afnan Tolah, Rawan Al Yahya, and Adnan Alsadah; professors from NC State including Dr. Venkateswaran Narayanaswamy, Dr. Alexei Saveliev, Dr. Kenneth Granlund, Dr. Kevin Lyons and Dr. Tiegang Fang; several individuals from the NC State Environmental Health and Safety Office including John Collins, Madhi Fahim, Ken Kretchman, and Will Rowland; The NC State Fire Marshal's office including Jon Brann, Greg Brooks, Kristen Boggs, and Bill Stevenson; staff with the NC State MAE Department including Martin Chiogna, Elizabeth Baker, Steve Cameron, Gary Lofton, Julia McLean, Toni Rand, and Jill Whitfield, and all my family and friends who assisted with this work.

TABLE OF CONTENTS

LIST OF TABLES

LIST OF FIGURES

1. INTRODUCTION

One of the most fundamental areas of research in combustion science is the creation of a flame through spark ignition in a fuel mixture. This phenomenon can be observed in both everyday scenarios such as driving an automobile, as well as larger-scale military applications such as flying an F/A-18 Hornet aircraft. Both applications rely on the same general concept: A small packet of energy is created (usually from a sparkplug) within a combustor filled with fuel (Figure 1). This energy raises the local temperature of the fuel to its adiabatic flame temperature, forming an ignition kernel that propagates outward into the mixture for a sustained flame and successful combustion [1].

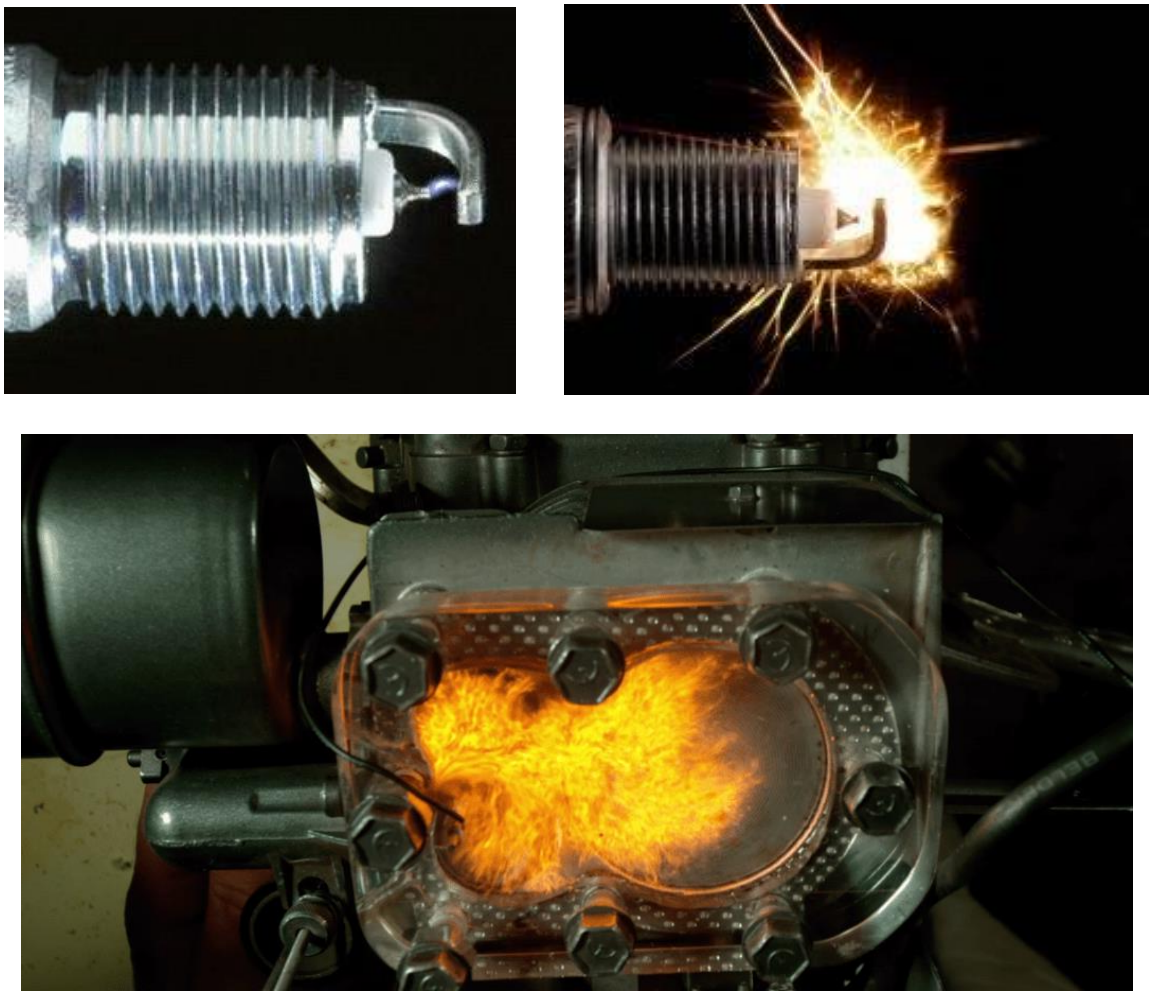

Figure 1. Spark ignition is one of the most fundamental methods of combustion, where an electric spark is generated (top left) to trigger a chain reaction of events (top right) leading to combustion of a fuel mixture (bottom) [2,3,4].

A growing area of research is being conducted in defining the optimal location and energy amount that must be deposited for a combustion flame to be produced (Figure 2). Determining the ignition probability is one of the driving factors for ushering in an era of cleaner-burning, more reliable combustion process. Predicting the optimal location and energy quantity of the ignition kernel has the potential to reduce the overall required energy for ignition at most flight conditions in military aircraft. Finding the successful ignition parameters at flight envelope conditions can be used as a roadmap for expanding the operation envelope of the aircraft in the near to mid future [5].

Figure 2. In order for successful ignition, three criteria must be met. The flame requires an oxygen supply, a fuel source, and energy or heat to ignite the mixture [6].

Currently, engine re-ignition likelihood imposes operation envelope limits – one of the primary goals for this investigation. Existing models use lean blowout (LBO) empirical correlations to predict ignition likelihood – these models assume global extinction parameters, based on global conditions (such as, blowoff always occurs at a certain high flow rate). However, the correlation between blowout and ignition physics is not fully understood and this correlation may be simply speculative. There is also work underway to develop Large Eddy Simulation (LES) models for capturing the ignition likelihood of turbulent flows [1,7].

Further ignition probability research is needed for designing the next generation of ignition systems in turbines and aircraft combustors. To date, current research has focused on gaseous fuels such as methane or ethylene. Liquid fuels (diesel) or jet fuels (JP-8) are just being

introduced to research experiments, mainly as laminar flows at low flow rates and small Reynolds numbers for the time being. According to E. Mastorakos, “Spark ignition of turbulent, nonpremixed combustion has not been studied as extensively as spark ignition of premixed mixtures either flowing or inside a combustion vessel.” [1] Nonpremixed describes fuel and oxidizer that only meet in the combustion zone; there is no prior mixing of the two substances. In a real-life scenario, turbulent nonpremixed ignition is exactly the type of flows encountered in aviation gas turbines or industrial burners. Turbulent flows induce an element of randomness into the air/fuel ratio and mixture composition at the spark location that requires laboratory testing to achieve an accurate mapping of the phenomenon. Additionally, the presence of turbulence in general can lead to straining of the flame kernel that may extinguish the flame and cease ignition [5].

Overall, the US Department of Defense is moving towards using one fuel source for all its vehicles, aircraft, generators, etc. This is termed “One Fuel Forward” or Single Fuel Concept (SFC) and has been discussed in concept for several decades, yet there is still progressing to be made towards achieving this. Unifying across all branches would mean that the selected fuel must have a long shelf life, so it can safely be stored unattended for long periods. However, there is a tradeoff that comes with this, as the fuel typically will need a larger energy source to cause ignition (Figure 3). These statements corelate to a fuel with a low flash point. Gasoline for current automobiles has a flash point of 233 Kelvin, while the primary fuel used for this initiative – kerosene based JP-8 – has a flash point of 333 K. The reason for using JP-8 over gasoline is chiefly due to this factor [8].

Figure 3. The military has a need for one unified fuel that can withstand the harsh environments faced at a forward operating base [8].

For example, because heavy fuel has a much lower flash point, it can be left unattended at a forward operating base or on a ship overseas without degrading its container and presenting a low flammability risk. For this project, initial testing was performed with other heavy fuels. Specifically, diesel fuel was used for initial experiments then the setup was switch over to Jet-A, an aviation fuel similar to JP-8.

Diesel fuel is very similar to jet fuel – in fact, some diesel engines can run with jet fuel replacing the diesel, however fuel efficiency does suffer due to the slight differences in energy content required for combustion between the two fuels. A diesel combustion engine may potentially be less environmentally-friendly than a "avgas" (aviation gas) engine due to higher compression ratios for ignition, which in turn produces more NOx (nitrogen oxide) pollutants. In terms of the physical chemistry, jet fuels tend to have a higher sulfur content (up to 1000 ppm) which makes the fuel "dry" or less lubricative. In contrast, diesel fuels are usually more viscous and contain special lubricant additives to promote healthy engine function. lubricated during normal operation. Thus, Jet-A can cause more wear on fuel injector systems. Testing of ignition probabilities for these fuels and others in the laminar regime offers useful data that can be extrapolated to more real-life (i.e., turbulent) conditions, but physical testing of turbulent flows is necessary to validate these claims (Figure 4). A longer-term goal is to move towards high-altitude scenarios for spark ignition, which would require testing of low-temperature fuels in order to find spark ignition probabilities for future use.

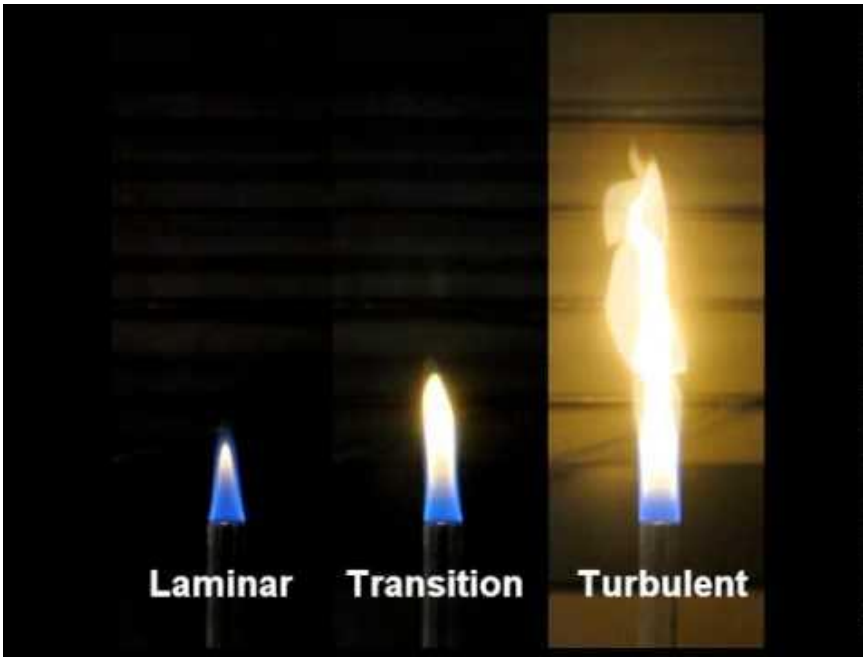

Figure 4. Evolution of a flame from laminar to turbulent [9].

Spark ignition testing presents a challenging task, because of the high energy needed to ignite heavy fuels, in addition to the fact that the spark kernel itself may be placed in a region where the fuel/air mixture is outside the rich or lean flammability limits of the mix. This requires precise placement of the spark in an ignitable zone of a nonpremixed, turbulent jet [3]. Furthermore, lean-premixed-prevaporized (LPP) engines and turbines where fuel is ignited at much leaner equivalence ratios are growing more common. These systems avoid autoignition in favor of forced ignition, which is necessary for the leaner mixtures. LPP systems reduce emissions due to regulatory and industrial standards, so the possibility of knowing ignition probability rates for these lean systems is of utmost importance. Studies have found that due to the lean, dilute nature of the fuel mix, forced spark ignition near the jet burner centerline is preferred for combustion [10].

2. PRIOR WORK

Previous work relevant to this project has been performed in many areas of spark ignition combustion. Experiments by several researchers including E. Mastorakos, D.R. Ballal and A. H. Lefebvre served as the foundation for understanding the spark ignition process and developing systems for measuring the probability of successful combustion for many types of fuels.

2.1 Turbulent Spray Flames

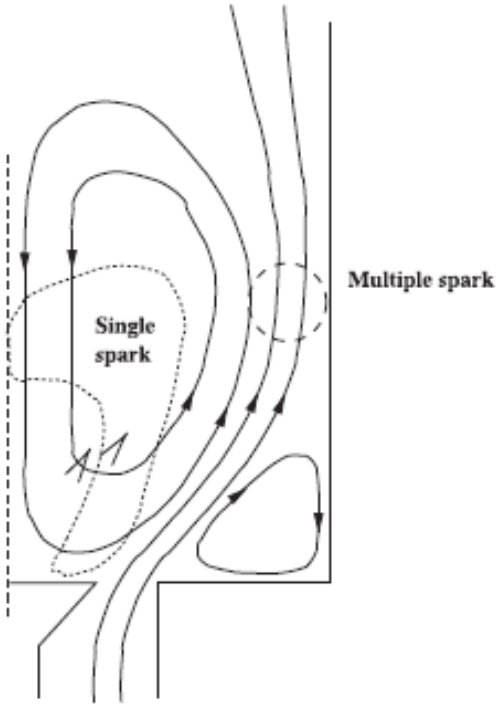

Figure 5. Cutaway view of Mastorakos' burner unit, detailing where a single spark was sufficiently effective to ignite the fuel mixture. Farther out near the walls of the chamber, multiple sparks were required for ignition [11].

Significant work has been performed by E. Mastorakos regarding ignition of turbulent mixtures, including both gas and liquid fuels (Figure 5). He defined forced ignition as using any externally imposed way to begin combustion – this can be through an electrical/laser spark, plasma jet, etc. In contrast, "autoignition" occurs when one or both of the reactants (fuel or

usually just the oxidixer) are already at a high enough temperature for chemical reactions to begin and initiate a combustion event. Forced ignition is therefore useful in that the initial conditions are essentially “chemically frozen” and the spark provides a way to increase the temperature of the mixture above the autoignition temperature significantly and rapidly.

For liquid spray flames, there are three distinct stages in spray flame ignition: 1) kernel generation, 2) flame growth, 3) burner-scale flame establishment. These stages are universal and true for premixed, nonpremixed, swirl, nominal, and spray flames. Stage #3 is where ignition probability has importance, and forced ignition can be experimentally tested to collect data on ignition results. An ignition map can be made from the data, showing most likely points of successful ignition given a forced ignition spark.

However, the spark ignition event itself is very complex and can be broken down further into several modes for both fire/misfire cases. These are: (a) successful combustion through spark ignition, (b) the “short-mode” failure, (c) “long-mode” failure, and (d) blowoff failure. Mode (a) is the only case representing a successful ignition firing, while the other modes represent either unsustainable ignition or a complete misfire. Short and Long mode failures occur when the spark deposits an insufficient amount of energy (below the minimum ignition energy, common for spray combustion) or the spark is deposited in a region where there is low ignition probability. Blowoff failure can occur if spark is in a lean region of the mixture or the exit jet velocity is too high to anchor the flame. These blowoff events typically occur on the scale of milliseconds, whereas a laser pulse can be trigged on the nanosecond or microsecond scale.

This is a clear benefit for using laser forced igntion over sparkplug-based systems: Lasers offer much more flexibility in defining the spark location, pulse energy, and pulse duration. At right is an ignition profile map detailing where a single spark is needed to create igntion, while farther out into the lean mixture multiple sparks are needed. Laser ignition offers the ability to test several spark locations in both regimes through precise focusing of the beam. In contrast, a sparkplug or electrode spark gap system can create flow blockage that may impact the ignition results [11].

2.2 Ignition Energy

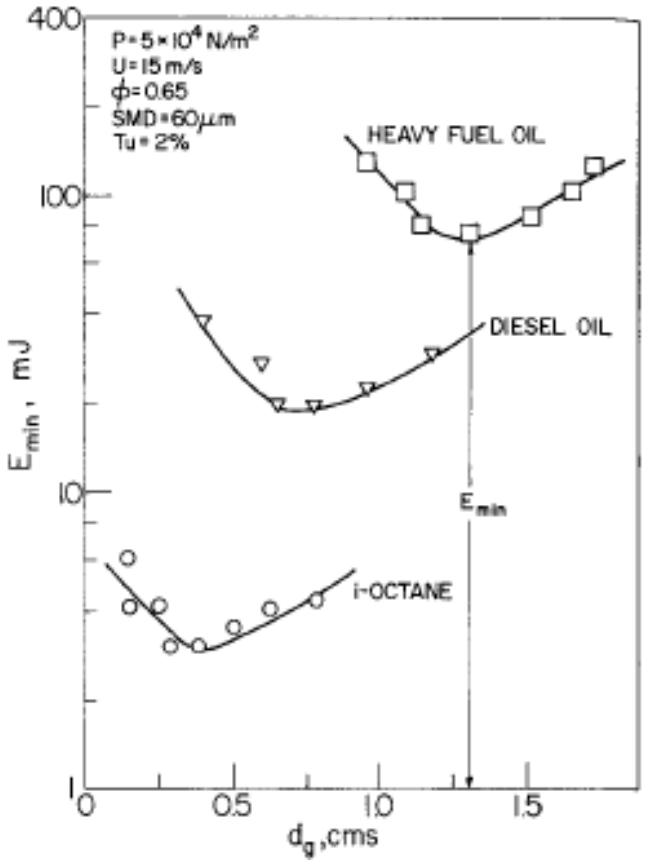

Figure 6. Diagram from Ballal and Lefebvre showing the minimum ignition energy versus electrode gap width. Their experimentes used electrodes spaced apart at diferent distances. For heavy fuels, around 100 mJ of energy is needed [12].

D.R. Ballal & A.H. Lefebvre have performed extensive research on the ignition process itself. Their work details the energy needed for successful ignition of the fuel mixture (Figure 6). Ignition of heterogeneous fuel-air mixtures was investigated assuming 1) infinitely fast chemical reaction rates and 2) the sole criterion for a "successful" ignition is an adequate concentration of fuel vapor in the ignition zone. This experiment used an electrode spark gap system to achieve ignition. Using heavy fuel oil, diesel, and iso-octane, they used a spark ignition setup to plot ignition energy vs electrode gap width at right. Experiments showed the importance of mean drop size on minimum ignition energy for all cases (smaller droplet size requires a higher ignition energy). Additionally, the presence of fuel vapor can reduce the

minimum ignition energy, which is especially true at larger droplet sizes. Experimental results do not match theory for certain cases (low pressure or low equivalence ratio) because fuel vapor may be present before the spray (the mixture is not fuel droplets and air only) and chemical effects were neglected for this study. Overall, heavier fuels need a higher ignition energy to achieve successful combution compared to lighter fuels such as methane or ethylene [12].

2.3 Laminar Fuel Injectors

Additional work by Ballal in a follow-up study investigated spark ignition of fuel sprays such as kerosene and diesel. For this, the fuel was atomized into fine droplets using a swirlex atomizer and then injected into the combustion chamber. They had already optimized the spark energy and duration from other studies, then applied their methods for a range of fuel droplet sizes from 20-1280 micron Sauter Mean Diameter (SMD) (Figure 7) [13,14].

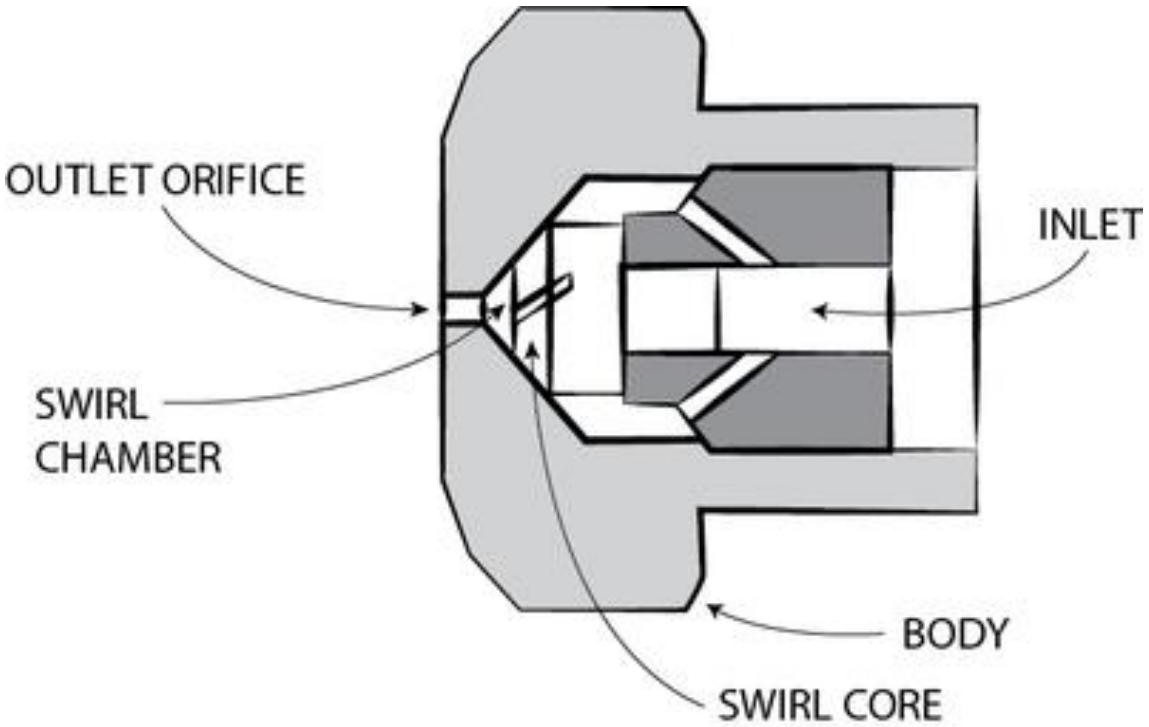

Figure 7. Diagram of an atomizer nozzle. Flow is injected moving from right to left and passes through swirling vanes, creating fine droplets at the orifice [13,14].

Additional work in this field by Cochet investigated 2-phase flows, where atomized liquid fuel was evaporated by heated air in the combustion chamber [15]. Nitrogen has also been used as a carrier gas to evaporate fuel flows, as demonstrated by Shelby (Figure 8) [16].

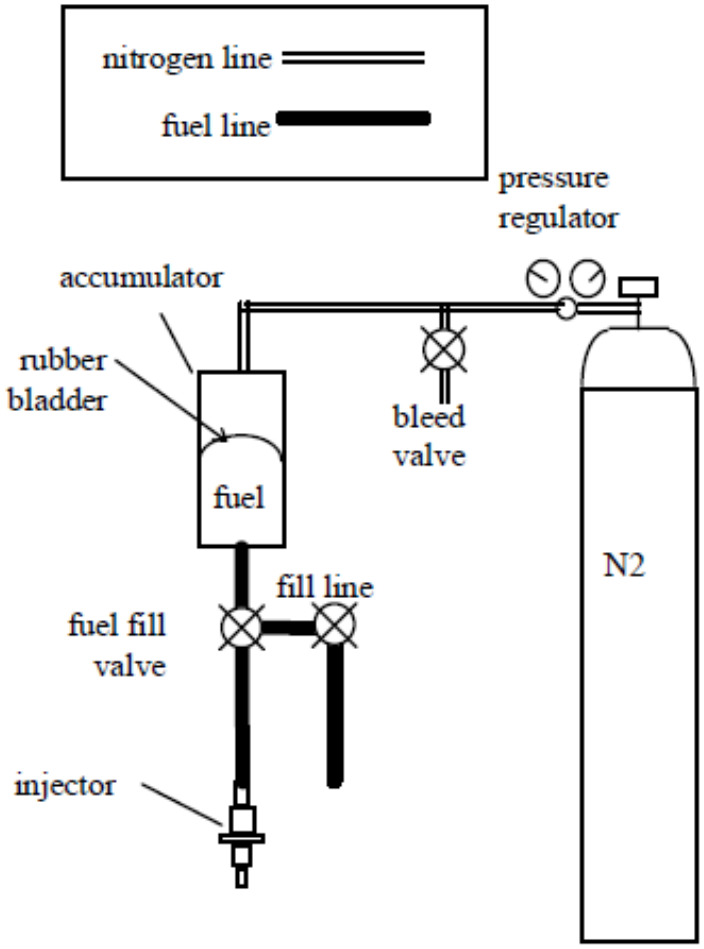

Figure 8. Diagram of Shelby's experimental setup, where nitrogen is used as a carrier gas for the fuel [16].

These are generally nonpremixed flows because the fuel nozzle atomizes the fuel at the orifice before it mixes with the carrier gas. However, fuel sprays take additional energy in order to ignite. Some of the spark energy is required to change the fuel phase from liquid to gas and then into plasma during the combustion process. An alternative method is to use prevaporized fuel, where the fuel is already in its gaseous state when mixed with the carrier gas for combustion experiments. This gives a more realistic perspective on the amount of spark energy needed for combustion, because the phase change variable is removed. These experiments are also a closer match with the LPP engines used for industrial settings [17,18,19].

For prevaporized fuel injectors, syringe injectors are commonly used. These pass liquid fuel (kerosene or Jet-A) into heating coils and eventually to the burner unit. Romero's setup in Figure 9 details the fuel injection and temperature monitoring system that was used [20].

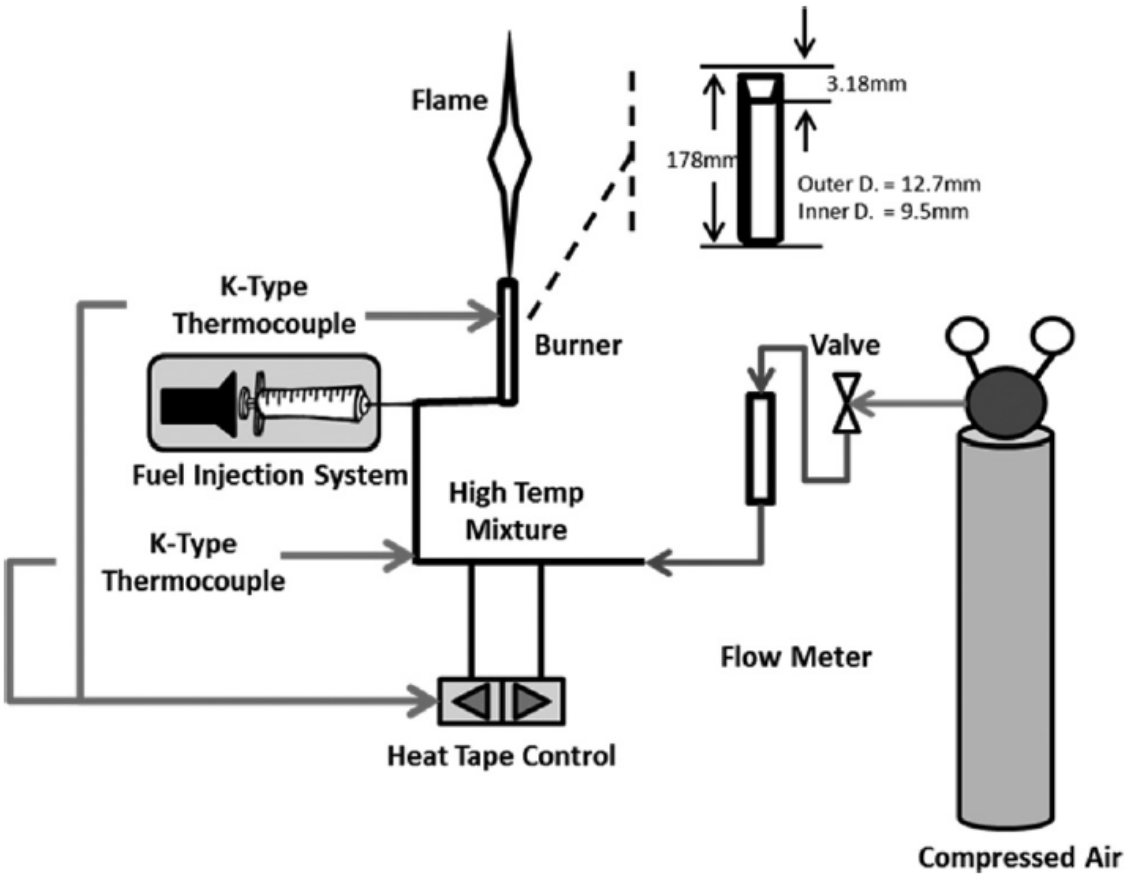

Figure 9. Experimental Setup for Romero's work, using a syringe fuel injector and heating tape to prevaporize the fuel [20].

Once the fuel has been vaporized, conventional spark ignition experiments can be conducted at the burner. Current LPP research has focused on initial studies with laminar flows at low fuel flow rates [21, 22, 23]. Commonly the liquid fuel is diluted with nitrogen at a 10:1 ratio by volume, with some fuel-rich experiments using 5:1 or 6:1 dilution ratios [24, 25, 26, 27]. The fuel is injected at low flow speeds to keep the system behaving laminarly, usually at 1 liter/hour (LPH) or less [28, 29, 30, 31]. Further investigation is needed to expand the scope of these efforts into the turbulent regime at higher flow rates.

2.4 Research Motivation

The work of Mastorakos, Ballal and Lefebvre provided a baseline set of procedures and experiments for analyzing the full capabilities of a spark ignition system. There has also been substantial work in understanding small scale, laminar flows for ignition experiments. In practice, experiments with turbulent fuel mixtures are typically performed in large-scale industrial burners. So, the motivation behind this project is to bring together all these research efforts. The goal of this project is to determine how can heavy fuels be used for spark ignition experiments on a small scale, in a laboratory setting, at real life (turbulent, nonpremixed) scenarios.

3. EXPERIMENTAL METHODS

To perform the experiments and collect the data required, several experimental methods were followed. A detailed description of the apparatus is also included.

3.1 Laboratory Facilities

Experiments for this project were conducted in the Turbulent Shear Flow Laboratory at NC State University in Raleigh, NC. This lab includes three facilities for combustion and turbulent flow research experiments. Initial tests and intermediary work was performed in the High Pressure Combustion and Laser Diagnostics Lab, while the full experimental setup was eventually moved into the Reacting Flows and Turbulent Jets Lab for data collection. Both facilities are kept at an ambient laboratory pressure that is slightly below atmospheric pressure (-0.004 in. wc), to provide a positive draft inside the facility and eliminate leakage of combustion products into the main building.

3.2 HVAC Modifications

In order to prevent leakage of fuel during this experiment, a custom-fitted steel panel was added to the top of the combustion exhaust canopy. This extended the canopy paneling down to the minimum possible height above the experimental setup in order to prevent any fuel leakage into the main laboratory. Additionally, aluminum tape was used to seal any gaps between the panels of the hood (Figure 10***)***.

Figure 10. Exhaust Hood Modifications before (left) and after (right).

Figure 11. AirFlow Instruments Velocity Meter (left) and Wizard Stick (right) used for flow rate measurements and visualization experiments.

Measurements showed that even with the additional paneling, the exhaust flow rate at the experimental setup was insufficient to capture the flow due to the vertical distance from the duct down to the burner unit (about 3 m). Measurements were taken with an Airflow Instruments Velocity Meter TA440. It was found that the plane of the duct exhaust was originally set at 200 cfm suction into the building exhaust while near the burner the reading was essentially stagnant air. A Zero Toys Wizard Stick instrument was used to visualize the airflow in this region before experiments were performed (Figure 11). This device uses a

glycerin vaporizer to produce a white vapor that dissipates into the air as a flow visualization test. To solve this, extension ducting was added to connect the top of the combustion hood directly to the burner setup. This substantially increased the flow rate at the burner plane to over 800 cfm (Figure 12). The experiment had a prescribed jet velocity of up to 50 m/s, and the additional ducting setup was able to account for half of this due to buoyant forces.

Figure 12. Exhaust duct modification to connect burner with ventilation.

Visualization testing of the glycerin with this setup is shown at right. This setup was sufficient for lighter fuel experiments with methane or different intermediary testing with air and nitrogen. However, experiments with heavy fuel required further modifications. One possibility during the experiments with prevaporized heavy fuel was that the fuel would recondense on the walls of the ducting or the vapors may collect further up in the exhaust system, causing risk of an explosion or fire in the building. To solve this, the additional ducting was removed for prevaporized fuel experiments. The additional paneling was left in place to contain the fuel vapors within the combustion hood (Figure 13).

Figure 13. Visualization of glycerin testing with additional ducting modifications.

3.3 Incinerator Attachment

A secondary incinerator flame attachment was added above the main experimental setup to burn off any excess fuel vapors. This attachment was not fixed on the burner unit; rather, it was freely resting on support struts above the experimental setup.

Figure 14. Methane incinerator attachment.

In case of a pressure buildup or explosion within the combustion zone, the incinerator attachment can freely move up and allow the pressure to vent out if needed. A full description of the incinerator attachment is included in 3.4 Experimental Setup. Once this was added, further modifications were made to the laboratory exhaust so that the velocity meter measured over 1,000 cfm of suction at the plane of the exhaust and about 200 cfm at the plane of the burner, while keeping 250 cfm through the laboratory gas cabinets in case of an explosion event in the cabinets. These readings were verified on the electronic flowmeters built in to the building ducts.

Finally, an additional power outlet was added to the laboratory to accommodate the heating unit for prevaporized experiments. The facility contained a NEMA L 6-20 (240V, single phase) outlet for the laser system. An additional outlet was installed because both the laser and heater

must be in use for the experiments. The outlet was strategically placed near the combustion hood to decrease the amount of wiring needed to connect the heating components to the outlet.

3.4 Initial Experiments

The Turbulent Shear Flow Research group has performed significant work with combustion and turbulent flows. In particular, recent experiments with methane ignition served as the foundation for this work with heavy fuels. These trials used both premixed and non-premixed fuel injectors. The non-premixed jets create a diffusion flame, where the only air to sustain combustion comes from air coflow surrounding the fuel jet. Premixed flames include a fuel/air mixture coming through the center jet. Additionally, these methane experiments investigated both room temperature and cold (230 K) ignition probability cases with the intent of expanding this work into heavy fuel ignition as well.

3.5 Methane Experiments

Prior experiments were conducted for several Reynolds numbers over both laminar and turbulent cases of methane flows. These experiments studied the effects of laser spark ignition at several locations radially outward from the burner jet, for fuel compositions from lean through stoichiometric to fuel rich. Table 1 shows the different mixture configurations used for these experiments, in both room temperature and cold (230 K) trials [32].

Table 1. Experimental Conditions for Methane Experiments [32].

Case	Re_D	% Air by Volume	U_j (m/s)	$U_{co\ flow}$ (m/s)
1086D	1086	0	2.9	0
R1086D	1086	0	2.0	0.2
R5780D	5780	0	15.7	0.2
R5780X30	5780	30	14.9	0.2
R9500X30	9500	30	24.5	0.2

In the chart, Re_D = 1086 represents a laminar flow speed while Re_D = 5780, 9500 are turbulent. Cases with a 0% air by volume are diffusion non-premixed flames while 30% air by volume is premixed. U_j represents the flow speed at the jet and U_{inf} is the air coflow velocity. For these experiments, the ignition probability (fire/misfire percentage) maps have been created in Figure 15. These plots show the ignition fire probability versus radial location away from the jet exit (r) divided by the jet exit hydraulic diameter (D=6 mm). For these charts, several hundred tests were conducted and averaged over 100 shots fired to obtain the ignition percentage out of 100%.

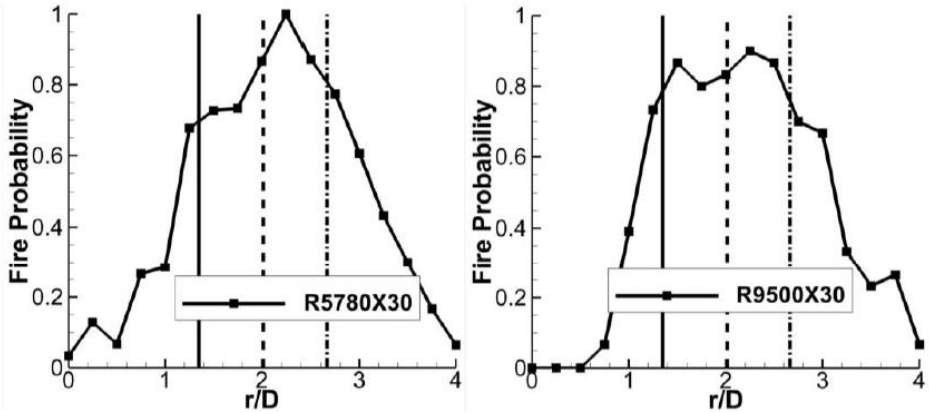

Figure 15. Ignition Probability Maps for Methane Experiments. At left is Re_D =5,780 and at right is Re_D=9,500. Overlaid on the plots are the r/D radial locations of the rich (solid), stoichiometric (dashed), and lean (dash-dot) limits [32].

Shown here are the two room temperature turbulent premixed cases. As it can be seen, the peak ignition likelihood is near stoichiometric on the lean side, farther away from the burner. For the cold cases, it was found that at 230 K the flame kernel propagation speeds are reduced. Ignition is less likely at equivalent input energies for both lean and rich regions. However, the ignition rate is near equivalent in the optimal region is nearly equivalent for the cold and room temperature cases. This may be due to the presence of an ideal mixture at stoichiometric conditions, allowing some local regions (such as at the center of the laser spark) to reach the adiabatic flame temperature quickly and begin forming the flame kernel that propagates outwards. Non-ideal cases have slightly different temperatures that must be reached for combustion and may not occur in local pockets as frequently for colder mixtures.

Flame Luminosity and CH* Radical imaging was also performed. Shown here are two samples, both taken for the Re_D =5780 turbulent premixed case, near the stoichiometric location.

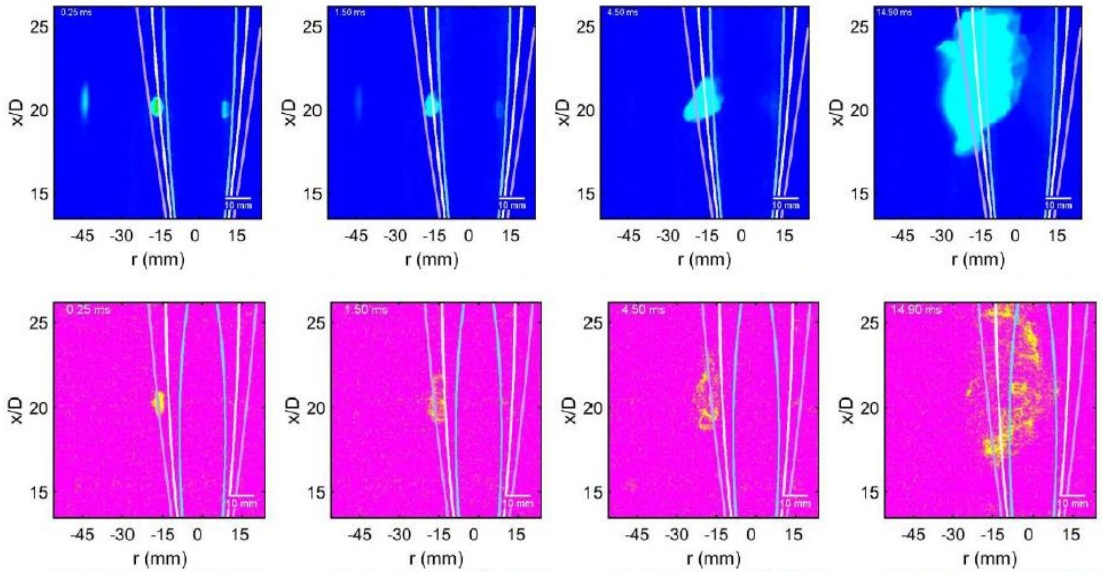

Figure 16. Flame Luminosity (top) and Chemoluminescence (bottom) of ignition near the stoichiometric location. The luminosity profile shows the flame kernel development over time, while the CH* radical provides an indication of the flame front [32].

The absorbed spark energy for methane was also studied. The absorbed energy profiles at several Reynolds numbers are shown below. These show an overall decreasing trend as the spark is moved axially away from the burner.

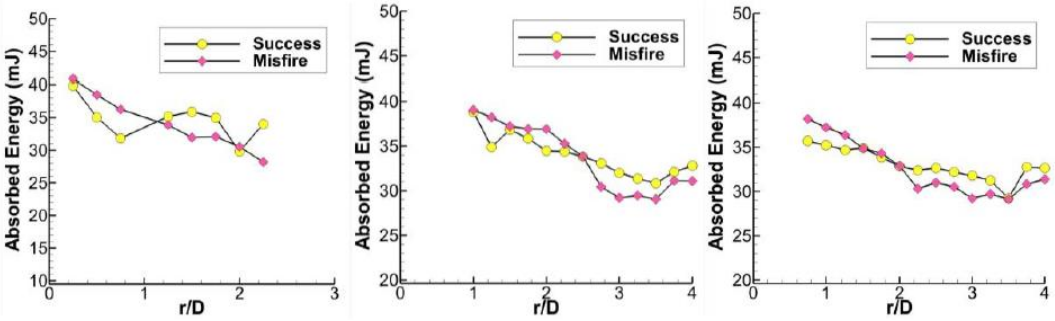

Figure 17. Radial profiles of absorbed energy by the spark versus radial location outward. From left to right: ReD=1,085, 5,780, and 9,500 [32].

To compare these results taken through laser ignition with a spark plug system, a validation study was performed in Figure 18 below [32]. These results show a strong corellation that laser spark ignition results should compare favorably with spark gap experiments based on the ignition probability at matching energies.

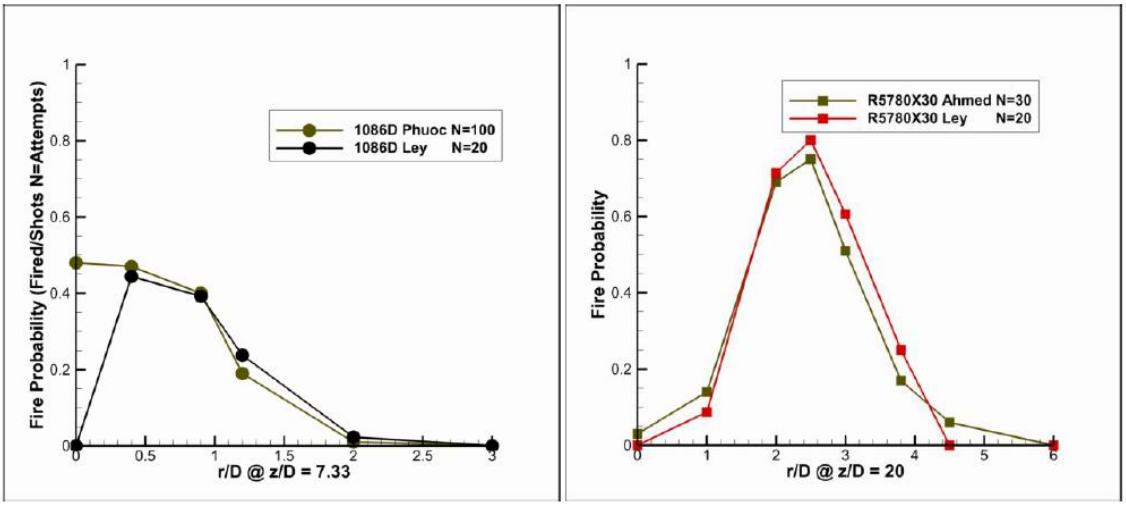

Figure 18. A validation study was performed to evaluate the correlation of a laser spark with an electrode gap spark system.

Overall, these methane experiments showed that the highest ignition probability occurred near stoichiometric conditions – slightly on the lean side of the mixture. Outside of the lean and rich flammability limits, the ignition probability was non-zero (consistent with prior research). These tests provided a baseline recreation of Mastorakos & others' spark ignition experiments at real-life operating conditions (i.e., cold) for ignition scenarios. The next step from here was to work towards ignition of heavy fuels.

3.6 Experimental Setup

Heavy fuel experiments were performed using a modified Jet in Coflow (JICF) buner. The original JICF burner used for methane experiments is shown below in Figure 19. This consists of a plywood cylindrical hollow tube, with 165 mm outer diameter. The plywood was laser cut from large sheets into thirds of the circle, in order to reduce material usage. Plywood was used rather than metal to reduce weight so that the entire burner assembly can be moved using a linear stage below. These plywood sections were then glued together to make the full cylinder. Aerogel and foam insulation layers were added to prevent temperature losses during the experiment. Additionally, a side port was added into the side of the cylinder for air coflow. This was insulated with PVC piping and aerogel insulation, then a ½" pipe fitting was attached to the exterior for the airflow.

A honeycomb ceramic flame arrestor was placed on the top, to straighten the air coflow and prevent flashback into the mixing chamber. Once built, the system was tested for leaks through the plywood/insulation and the design was found to be sufficient and sending the desired flow rates with negligible/no leakage through the walls of the burner.

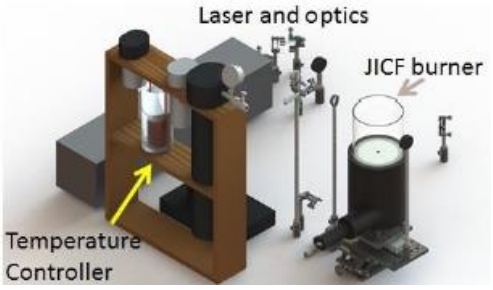

Figure 19. JICF Burner used for the methane experiments. Slight modifications were made for the heavy fuel experiments.

The new design features several edits to the above the setup, including the methane incinerator attachment and modifications to the temperature controller for prevaporized fuels. An original sketch of the incinerator design is shown below in Figure 20. The modified burner consists of a Jet-A / Nitrogen fuel injector for sending prevaporized Jet-A fuel mixed with hot nitrogen as a diluent (non-premixed fuel). This enters a combustion zone encased by quartz glass tubing, where the fuel meets room temperature coflow air. The quartz glass tubing is 457.2 mm tall, with an inner diameter of 155 mm and an outer diameter of 161 mm. The laser spark is also deposited within this quartz section.

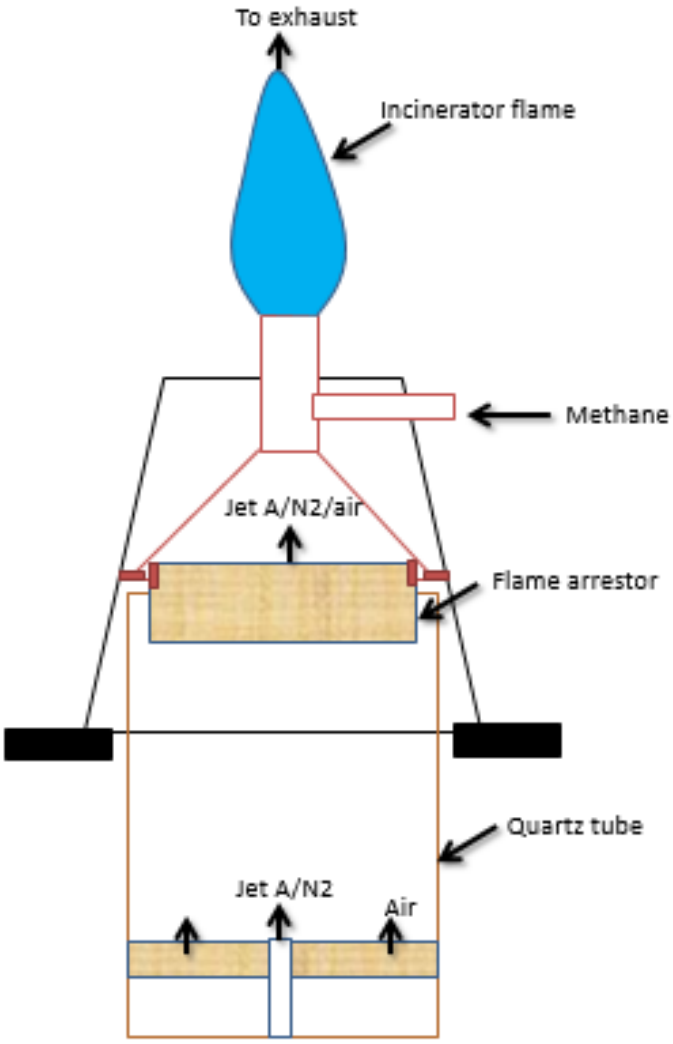

Figure 20. Methane Incinerator Drawing.

Figure 21. Top and bottom ceramic honeycomb flame arrestors.

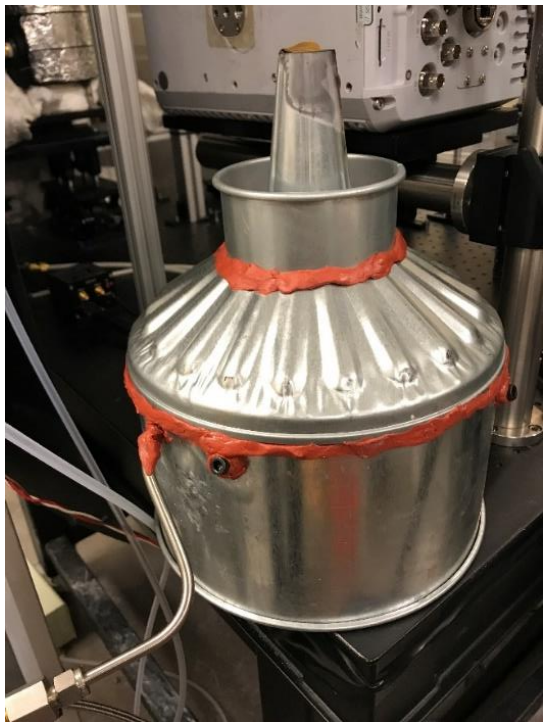

Figure 22. Methane incinerator with fire-stop putty to seal for leaks.

Above the setup is the methane incinerator flame, held steady above combustion zone. Flame arrrestors are placed at either end of the quartz tube to prevent flashback and quench the flame from either end (Figure 21). The flame arrestors are ceramic honeycomb structure with a cell density of 230 CPSI (cells per square inch). Each ceramic honeycomb is 2” in height. These were purchased from Applied Ceramics as 6” square pieces, then machined using a waterjet into the circular sections shown here with a 6” diameter. The honeycomb sections are suspended in place with a combination of fire-resistant putty and metal constraints.

The incinerator is placed on mounting struts, freely resting so as not to put weight on the quartz glass (Figure 22). The incincerator is not bolted down to the mounting struts, allwoing it freedom to raise up and away from the combustion zone if a pressure buildup occurs. For the experiments conducted, the fuel and air mixture is several times below the flammability limit in the combustion chamber. Therefore, the mixture is well below the eplosive limits as well. There are only a few possible locations within the chamber where the mixture will igntite, and that is what this project is hoping to explain.

This setup was designed to accommodate a mixture ReD = 10,000 at jet tube exit as a design constraint for turbulent flow measurements. To achieve that, the original center tube from the previous JICF burner (6mm inner diameter) was replaced. A ceramic tube was inserted through the bottom port of the burner and up through the flame arrestor to prevent heat losses from the fuel/nitrogen mix. A steel tube with an inner diamter of 1.5mm was inserted into this ceramic to provide the jet tube diameter needed to achieve the given Reynolds number at a known flow rate and flow viscosity.

The igntion spark was supplied by a Q-switched Nd:Yag laser (Continuum Surelite III-10) operating at 1064 nm wavelength. This laser produced a pulse 9.5mm in at a rate of 10Hz, over 10 second periods of testing. The laser's shutter system was designed with this 10 second limit in mind to accommodate a short fuel injection period over the same timeframe that was imposed as a design constraint. Additionally, this system prevented any pulse-to-pulse coupling that could influence ignition rates of the system. the probability of ignition. The 1064 nm beam was focused to the disured ignition location within the quartz tube to a focal spot was about 1 mm in diameter (which also represents the measured spark size). This laser spark was deposited at a fixed point in space so that the modified JICF burner could be remotely moved to achieve the desired spark location. This setup allowed the spark to remain focused at the same settings for every experiment.

Figure 23. Peristaltic Pump and tubing (left) and Jet-A liquid fuel tank (right).

Jet-A fuel was kept in a 2L fuel tank with one exit port. A petcock valve was threaded into the tank at the port and fuel lines were attached to carry the fuel into the prevaporizer system. Two additional valves, a needle valve for precise control of the flow rate and an on/off ball valve, were located downstram of the tank before prevaporizer system.

Additionally, a gauge was installed for measuring the fuel pressure and a three-way valve containing a plugged air line for purging the system of fuel if needed. The fuel lines chosen were chemical hose that meets criteria well above the expected ambient conditions for the liquid fuel. These fuel lines passed the Jet-A from the tank into a peristaltic pumping apparatus. A peristaltic pump is a positive-displacement pump used for pumping of various liquids. A rotor with several rollers compresses the peristaltic pump tubing, pinching the tube and forcing fluid upstream. As the roller passes and the tube returns to its undisturbed state, more fluid from the tank is forced into the pumping section. This process is called peristalsis and provides

an alternative to centrifugal pumps (Table 2). It was found that vaporizing the fuel upstream causes some fluctuations and cavitation which present issues for centrifugal and rotary vane pumps operating with liquid fuel. The peristaltic pump dampens out these effects because the flow is not separated through vanes or other mechanical methods to achieve the desired flow rates. The pump flow rates were measured for the full range of dial settings (Figure 24).

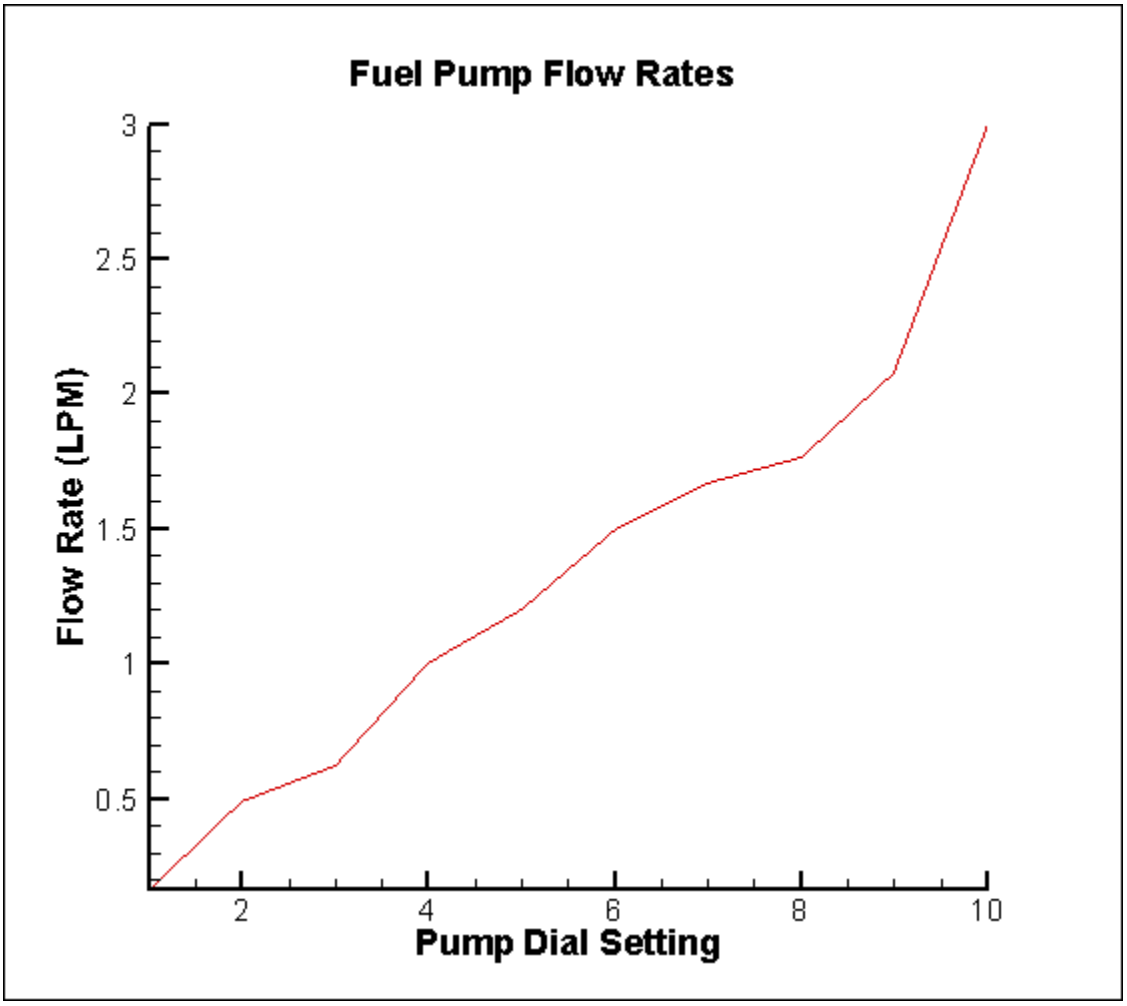

Figure 24. Calibration curve taken from measurements with the peristaltic fuel pump. Each dial setting on the pump corresponds to a certain fuel flow rate for the experiments.

Table 2. Technical specifications of the peristaltic pump and tubing.

Cole-Parmer Masterflex L/S Peristaltic Fuel Pump
Analog Variable Speed Control with Easy-Load Pump Head
Max Theoretical Flow Rate: 2.9 Liters/minute (LPM) Min Theoretical Flow Rate: 0.0012 LPM Max Measured Flow Rate: 3.0 LPM Min Measured Flow Rate: 0.16 LPM
<u>Peristaltic Pump tubing</u> Max Theoretical Pressure: 140 PSI Max Measured Pressure: 30 PSI
120V AC Power Supply, 1.5 Amp Current Draw 37 Watt Motor 1/20 Horsepower 20-600 RPM
670 Horsepower Theoretical Max

Once the liquid fuel passed through the peristaltic pump, it was sent into the prevaporized section. This consisted of 15 m of wound heating coils to raise the flow temperature above the boiling point. These coils were a combination of 304 stainless steel and copper due to their high heat capacity values (502 and 376 J/kg*K, respectively), wrapped with heating tape and wool insulation. The inner section was 5 m of coiled ¼" outer diameter copper tubing, wrapped with heating tape. This section was insulated with wool, then wrapped with 10 m of ¼" OD stainles steel coils to catch any heat losses. The fuel traveled from the pump into the steel section to slightly increase its emperature, then into the insulated copper section for vaporization (Table 3). After the fuel passed through the copper section, it was injected into the heated nitrogen stream and sent to the burner.

Table 3.Technical Specifications for fuel lines and fittings.

Fuel Lines
"Medium-Pressure Chemical Hose"
Max Theoretical Pressure: 500 PSI at 273 K
Temperature Range: 250 K to 350 K
Material: Nylon with Blended Rubber Cover
Compatible with stainless steel barbed hose fittings
Fuel Line Fittings *All Pressures at 273 K*
Pressure Gauge: 300 PSI Max
Brass Fittings: 250 PSI Max
Brass Needle Valve 200 PSI Max
Stainless Steel Fittings: 4,100 PSI Max

The nitrogen stream was passed from a tank through a mass flow controller and into an OSRAM SureHeat Jet Air Heater (3kW, 240V, 1-Phase, 12.5 Amps). This inline heater preheated the nitrogen to a set valvue of 500 Faehrenheit. The temperature was controlled with an OSRAM Control Panel that uses 2 internal relay circuits to supply a variable voltage to the heating coils so that they reach a desired temperature, as measured through a PID controller with thermocouple data transfer wires. The control box was powered through the new NEMA L6-20 outlet that had been installed in the lab. To run the heater effectively and prevent burnout, a minimum of 75 LPM of flow was needed through the inline heater. A tee valve was added upstream to switch beween air flow (for preheating) and nitrogen (for the experiments). The air ws never mixed with fuel as all upstream fuel vales were closed; the air went up through the jet burner tube and out into the combustion hood.

However, only a small amount of nitrogen was needed to run the experiments and achieve the desired Reynolds number and fuel/nitrogen mix in the combustion zone. Therefore, the hor nitrogen flow was teed off into a waste line and a fuel injeciton line. The waste line was

directed through copper cooling coils submerged in an ice bath to cool down the flow, then through another mass flow meter and valve system before venting out into the combustion hood. The fuel injection nitrogen line was immediately sent through a needle valve and mixed with the fuel injection port at a tee valve.Using the mass flow controller upstream before the heater and downstream in the waste line allowed precise control of the nitrogen flow rate at the injeciton port. The nitrogen lines were calibrated to acount for friction losses across all flow rates (Figure 25).

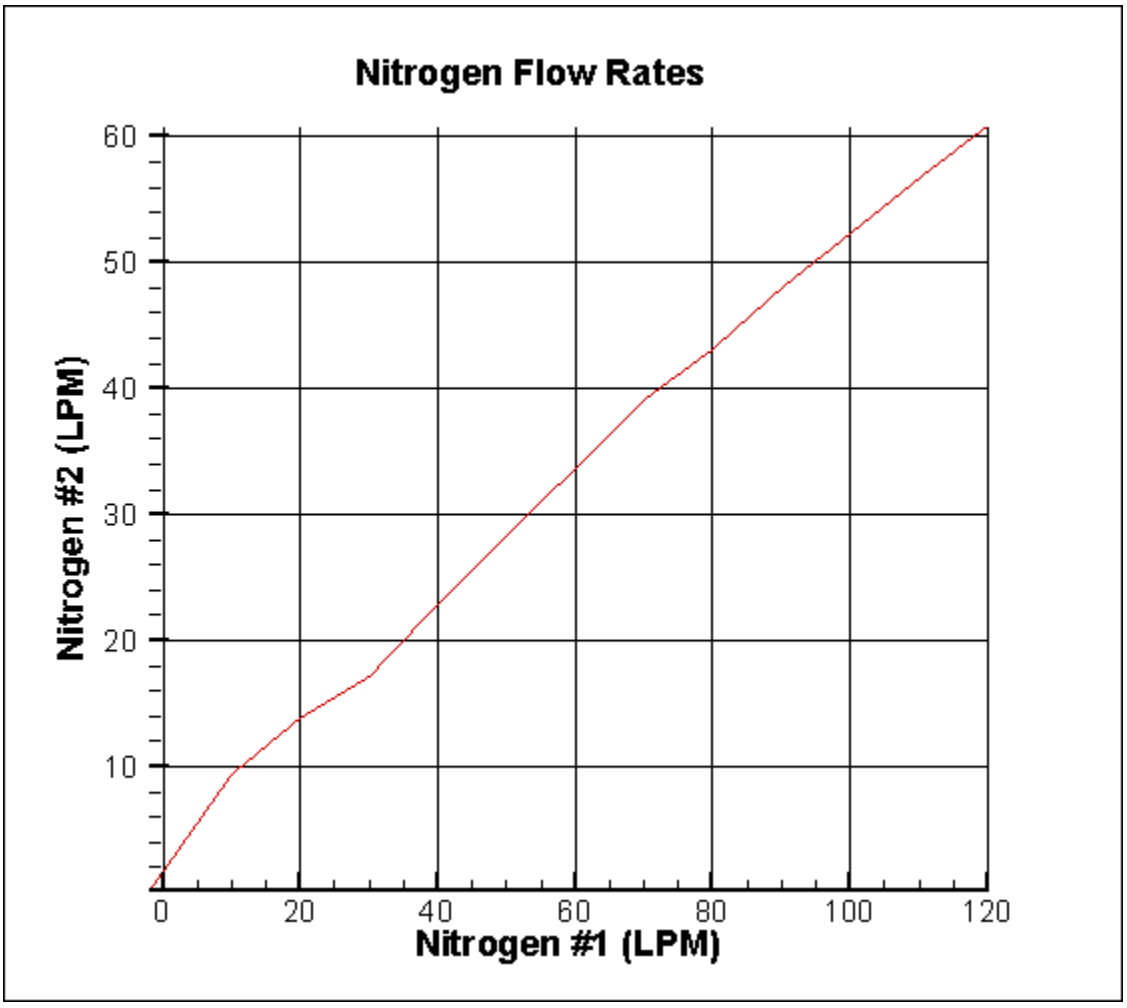

Figure 25. Nitrogen was measured at separate flowmeters to account for losses and calibrate the fuel injection line based on the differential flow rates.

Once mixed with the fuel, the nitrogen/fuel mix was sent through flexlible steel tubing intothe burner jet. Flexible tubing was used to ensure the burner still had free range of movement to

achive testing at several spark locations. The hot nitrogen lines were insulated with alumina ceramic blankets rather than the wool used for the fuel lines. The wool was ciruclar and allows coils to be wrapped around it easily, while the alumina is a blanket that can be wrapped around the pipe fittings, flexible steel tube, and other sections. Both provide sufficient insulaiton to keep the mixutre heated above the boiling point of the fuel.

Table 4. Insulation Technical Specifications

Wool Insulation	**Alumina Blanket Insulation**
7/8" Insulation ID, 0.02m Thick, 1m Length	0.02m Thick, 0.3m Square
Temperature Range: 0 to 922 K	Temperature Range: 0 to 1873 K

3.7 Experimental Procedure

Figure 26. Personal Protective Equipment (PPE) worn during experimentation.

To run the experiments, personal protective equipment (PPE) was required to be worn (Figure 26). A Nomex lab coat was always worn when experimenting with fuels for body protection. Closed-toed shoes and long pants must be worn also to prevent any skin exposure below the

lab coat. For facial protection, hooded/indirect vent splash goggles were worn for any work with liquid fuels. For ignition experiments, green laser safety glasses were worn to block the 1064nm spark wavelength. For experiments with the PIV laser (no laser spark), orange laser safety glasses were worn to block the 532 nm laser sheet. A face shield (with green laser goggles underneath as secondary protection) was used for any experiments with both fuel and the spark ignition laser. Nitrile gloves were worn when handling the fuel, fittings, tanks, etc. The gloves were replaced immediately if any breaks/breaches occur in the material. Gloves were always replaced after being worn for about 4 hours so that the fuel does not permeate the material, and properly disposed of. For any combustion experiments, fire retardant gloves were worn to protect from burns and heat.

First, the system was preheated to ensure that the metal and ceramic tubes had enough time to reach their steady-state temperatures at high enough values to sustain vaporized fuel experiments. Air was sent through the heater and through the jet tube to allow for this preheating phase while conserving fuel and nitrogen. The heater was set to 588 K, which provided a jet temperature above the vaporization temperature of the fuel after accounting for heat losses. This value was achieved in steps moving from 273 K up to 588 K at a rate of 50 K/minute to prevent voltage overload to the heater. The air flow rate was set to around 200 LPM to simulate the flow rates needed for the full experiment. A thermocouple was used to verify that the jet exit temperature and piping components reached the required temperature.

While the system was preheated, the laser was powered on and aligned. First, a visual inspection was performed to check that no equipment was in the laser beam path. All four laser shutters were check to make sure they were in the closed position. The room was prepared for laser experiments (safety curtain drawn, outdoor warning light illuminated, PPE worn), and the laser was turned on. The laser shutters were opened one at a time: 1) the physical gate on the laser equipment itself, 2) the internal laser shutter button, 3) the servo beam dump shutter, and 4) the pulse generator. This order was chosen to minimize risk of skin exposure in the beam path if an unexpected problem arose. to the servo trigger paired with the imaging equipment. Once the laser beam was fully opened, a small card was used to visualize the laser in the beam path and make sure all mirrors and lenses are in alignment. For this step, the laser was kept at a low energy level (80mJ). Once the alignment was verified, the laser energy was

increased so that sparks formed consistently (100-400 mJ) in a jet of preheated air surrounded by the quartz tube. The quartz tube needed periodic cleaning to ensure it allows the maximum possible amount of beam energy to pass through. Once sparks were formed consistently, the laser was kept on but all shutters were closed in the reverse order they were opened.

By now, the system had sufficient time to preheat, and the methane flame was lit on the incinerator. The methane safety valves were opened starting from furthest from the tank to the tank itself to prevent any pressure buildups in the fuel line as the tank was opened. Once fully, opened, the methane flow rate was throttled to 6.5 LPM (design constraint). Then the top flame was lit above the combustion zone. This was performed early in the procedure so that any fuel vapors will be burnt off as the fuel lines are opened for the experiment.

Next, the heated flow was switched from air to nitrogen. A three way valve system was used to split the air stream into coflow only and allow nitrogen to replace it on the line going into the heater. The flow rates were adjusted again to ensure the heater had above 75 LPM the entire time to prevent burnout. For experiments, the air coflow was set to around 185 LPM and the nitrogen flow rate was set between 90-120 LPM, giving between 60-90 LPM on the waste line depending on the valve position.

The fuel heater was turned on and sufficient time was allowed for the fuel to vaporize along the heating coils. Once the lines had reached the required temperature, the pump was turned on to start moving the fuel through the piping. Then, the jet valve was adjusted to a value that gave a consistent fuel/nitrogen stream at a well-controlled flow rate.

Once this was achieved, the laser shutters were reopened and a spark was produced in the combustion zone. If ignition was successful, an alarm system built into the servo shutter stopped the laser spark pulse generator to allow the flame to die out. If there was no ignition, the laser was left open to pulse at 10 Hz for a ten-second period. After ten seconds, the jet valve was closed for several seconds to prevent fuel buildup in the quartz tube. This process was repeated to collect the full ignition dataset. 100 laser pulses were given at each location to provide ignition probability percentage. The burner unit was periodically moved axially with a servo motion controller underneath the setup in steps of 1mm, to test ignition probability in several locations.

To shutdown the system, the fuel heater was turned off and the nitrogen heater was taken down to 273 K at the same rate of 50 K/minute. The laser shutters were closed and the laser turned off. Air was continually sent through the system until it reached room temperature to the touch and the heater could be turned off and all gas lines closed. The methane incinerator was extinguished last, to account for any traces of fuel that may have been present during the shutdown procedure.

For additional data collection besides the ignition probability map, particle image velocimetry (PIV) was performed to provide 2D two-component velocity fields at the spark location. Nanometer-sized alumina particles were seeded into the coflow air stream and the particles' laser scatter was imaged with a high speed camera. Sufficient seeing of the flow was achieved by seeding the co-flow and increasing its flow rate from 0.2 m/s or 200 LPM to 0.25m/s and 250 m/s. This increased flow rate was determined to not significantly alter the ignition phenomenon. The laser scattering images were processed using commercial software (La Vision Inc., DaVis 8.4) to provide velocity vector fields using a multipass algorithm that sized down from 64×64 pixels to 16×16 pixels with 50% overlap. The resulting vector fields had a spatial resolution of 0.25 mm with accuracy better than 0.01 m/s in the mean.

3.8 What If? Scenarios

To ensure safe practices were followed while performing these experiments, a "What If?" table was produced. This provided an outline of worst-case scenarios that could possible occur during experimentation and solutions to remedy or reduce the risk of each in Table 5.

Table 5. "What If?" Scenarios.

What if?	Answer	Probability	Consequences	Recommendations
Use on unventilated benchtop	Flammable vapors could accumulate and reach source of ignition fire	High	Extensive damage/downtime and costs	Use in fume hood
	Overexposure to toxic vapors	High	Adverse health effects	Use in fume hood
Mechanical failure of fume hood exhaust fan	Lack of exhaust but vapors still accumulate and ignition sources still present	Moderate	Adverse health effects	Suspend testing until exhaust is fixed or find a replacement hood in the adjacent lab for experiments
	Fire	High	Damage	Contain vapors as much as possible, take fire extinguisher safety class on proper usage
Power failure during use	Lack of exhaust, vapors may accumulate but at lesser magnitude, potential fire	Very high	Damage/health effects	Use manual shutoffs (ball valves, etc) in system design in addition to electronic switches
	Fuel flow rate is uncontrolled	Very high	Failed experiment, exposure to fumes/liquids	Wear proper PPE equipment to protect against splashes/fumes
Heater malfunction, electrical arcing	Possible fire in heating tape and ignition of solvent vapors	Moderate	Equipment damage/personnel injuries	Check electrical connections (plugs and wires); pretest heater before starting
Heater malfunction, supplies too much heat	Heat material above flash point	Moderate	Fire, damage, personnel injuries	Use fume hood so that vapors do not linger near exterior of heater

Table 5 (continued).

	Insulation or heating tape smokes or burns	Moderate	Personnel injuries	Do not leave unattended; check temperature of reaction at regular intervals and shut off if smoke is observed
Heater malfunction; supplies too little heat; if no heat, see loss of power above	Vaporization unsuccessful	Moderate	Liquid fuel spills at exit port	Point exit port down into fuel collection container to account for any unvaporized liquid fuel
Leak in Fuel Line	Spillage of liquid fuel	High	Fuel spills, possible fire hazard	Use PTFE tape and tighten all fittings before each new experiment; check for leaks by running the pump with heater off
	Escape of Vapors from fuel line	High	Fire hazard if near electrical components/heater	Tighten fuel lines prior to new experiments
Spill from hot collection container	Flash fire	High	Fire/damage/ personnel injuries	Do not handle hot vessel
	Vaporization unsuccessful	High	Lost time and materials	Do not leave setup unattended
Pump malfunction	Fuel flow rate is uncontrolled	High	Failed experiment, exposure to fumes/liquids	Wear proper PPE equipment to protect against splashes/fumes, use manual shutoff valves

Table 5 (continued).

	Electrical spark near fuel supply	High	Fire/Damage/ personnel injuries	Use barrier to shield power supply from fuel, keep pump elevated to prevent fuel spills on table underneath electrical equipment
	Electrical wires break	High	Lost time and materials	Ensure tight connections with strain relief for all wires, use electrical tape as needed
Fuel tank breaks	Flash fire	High	Fire/damage/ personnel injuries	Check container for signs of prior damage or use new container
Residual process gas in equipment when valves opened	Vessel breaks	High	Fire/Damage/ personnel injuries	Leave valves open for proper drainage after experiments and when not in use
	Vessel cannot be opened	High	Lost time and materials	See above
	Unintended reaction occurs	High	Hazardous byproducts	Conduct a review of all possible reactions and outcomes

3.9 Boundary Conditions

This work represents the experimental side of a comprehensive study to understand spark ignition of heavy fuels. A separate project is currently underway to investigate computational methods for simulations heavy fuel combustion to provide correlations with this experimental data. To achieve this, boundary conditions from these experiments were recorded and presented for use in the simulations. A summary of the relevant boundary conditions is presented below in Table 6.

Table 6. Experimentation Boundary Conditions.

Fuel-Nitrogen Mixture: Case 1: 4 LPM flow rate, 35 m/s jet exit velocity , 15:1 Nitrogen: Jet-A Dilution Ratio by Volume Case 2: 8 LPM, 50 m/s jet exit velocity, 30:1 Nitrogen: Jet-A Dilution Ratio by Volume
Jet Exit: 400K flow exit temperature Inner Diameter (*D*): 1.5mm Radial Locations: r/D = 0 – 4 in steps of 1 mm
Surroundings: Air flowing at 180 LPM for coflow Quartz Tube: 457 mm height (no influence by incinerator)
Spark: Spark size: 1 mm Location above burner: 35 mm in x-direction (x/D = 20) Energy: 100-500 mJ

4. RESULTS AND DISCUSSION

Several experiments were performed to conduct a full analysis of heavy fuel ignition. Overall, these represented the next logical step from the methane testing discussed earlier towards heavy fuel experiments at real-life scenarios such as high altitude, cold fuel combustion. The key findings are presented, then individual experiments are discussed and the results are presented.

4.1 Key Findings

It was found that three main factors contributed to the collection of data: 1) the temperature of the flow, 2) the phase of the fuel (liquid/vapor), and 3) the dilution rate of the fuel. A wide range of possible scenarios could be studied, however these experiments focused on specific temperatures and flow regimes. It was determined that there are several non-trivial locations where the fuel mixture will ignite when a spark is deposited, even well outside the lean flammability limits of the fuel. There are only a few possible locaitons within the combustion chamber where the mixture will ignite, and this project served to identify those locations through a parametric approach. Measurements for the burner setup were collected, including maps of the temperature profile, ignition probability, and mean velocity field. Additionally, individual measurements of the flame luminosity and chemiluminescence for successful ignition cases were collected. From this, specific parameter values for creating an ignitable mixture were determined.

4.2 Temperature Profile

Temperature profile maps were obtained by sweeping a thermocouple over the system while running at the experimental settings. A thermocouple was mounted on a linear stage and swept across the burner unit to obtain the values presented in Figure 27. The maximum measured temperature was 303 K at the spark height of x/D = 20, directly above the jet at r/D=0. As the profile shows, the temperature dropped substantially near r/D = 5 and settles at

ambient temperature near 297 K by r/D = 10. This provided a profile used for determining the experimentation area for ignition probabilities, so that the warmest portions of the flow were captured. Spark ignition experiments were conducted well inside the hot region, from r/D = 0 to slightly past lean, r/D = 4. However, of interesting note as that the flow temperature decreased from 400 K at the jet exit down to 300 K only a few millimeters above the jet. The surrounding air coflow was at 295 K, which may have been sufficient to cool down the jet flow significantly by the time it reached the plane of the spark location. Additional experiments with a new setup were able to increase the jet exit temperature to 533 K, well outside the distillation curve for Jet-A to ensure no liquid fuel was present at the jet exit plane. However, there was still a substantial drop in the flow temperature once the spark height was reached.

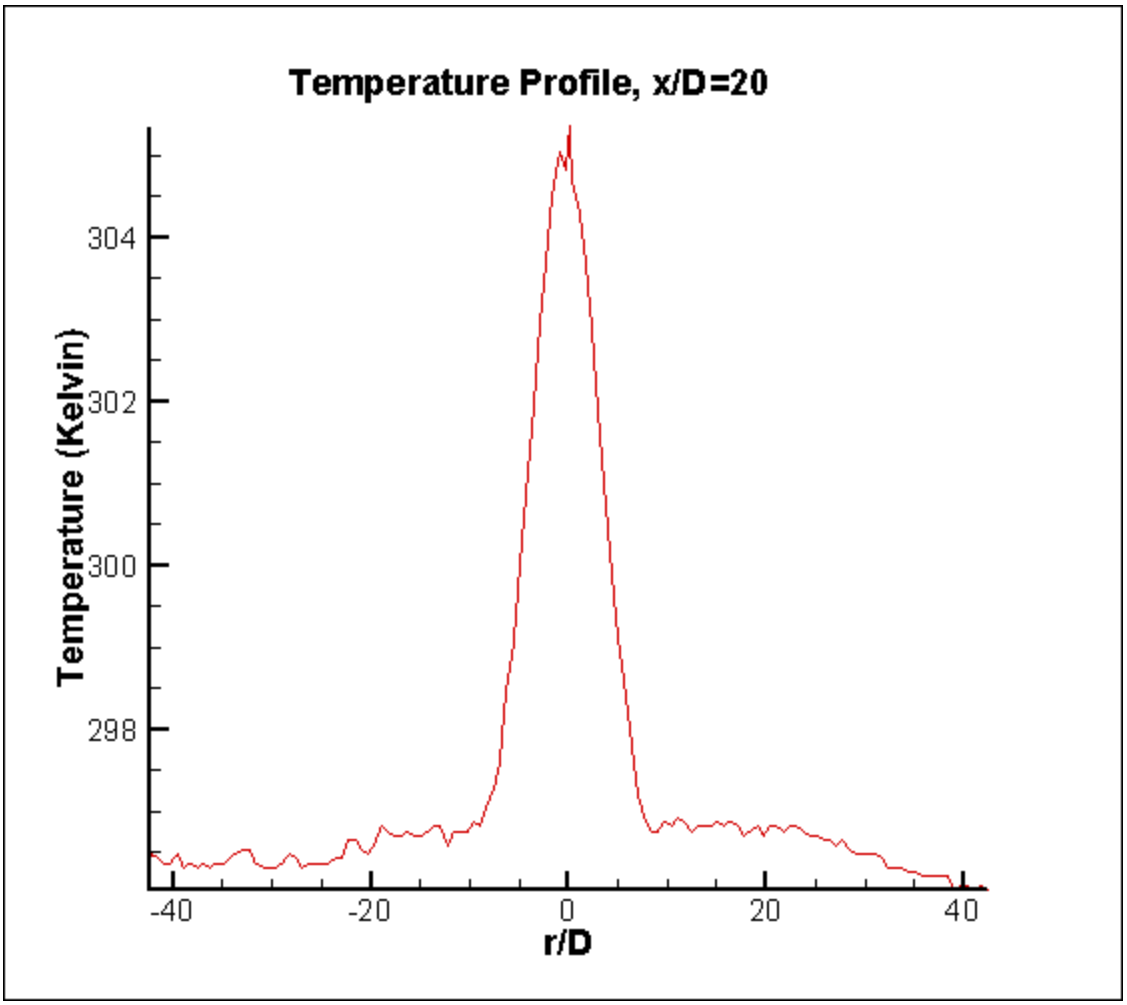

Figure 27. Temperature Map Profile at a spark height of x/D = 20, taken across the entire width of the burner from r/D = -40 to 40. The peak measured temperature was 303 K at r/D = 0.

4.3 Ignition Probability

Additionally, an ignition probability map was generated in Figure 28. This was collected at the Case 1 criteria of experimental conditions in Table 6. These experiments measured the flame ignition probability per 100 laser spark shots. Several hundred shots were fired and the results were taken over sets of 100 in repeated experiments to verify the ignition rates. The laser was set to 430 mJ for these experiments at a height of x/D=20 above the jet. Numerous trials were

run to obtain the probabilities over several hundred tests, and the results were averaged out per 100 shots. Overall, the probability trends held within 1-2% accurate at the higher probability cases between each set of 100 shots. It was found that the highest ignition probability of 14% occurred at r/D = 0, directly above the jet. Farther out, increasing r/D caused a decrease in the ignition until the mixture was well outside the lean flammability limits at r/D = 3-4. The stoichiometric location for this mixture is near r/D = 2.5, however the highest ignition probability was in the fuel rich zone. Some isolated experimental runs gave much higher ignition probabilities (up to 64% at near-stoichiometric locations) but these trials were not able to be repeated with enough consistency to draw any definite conclusions. This may be due to the dilution rate of the fuel – what is normally the fuel rich version may have closer to a stoichiometric mixture due to the dilution of the fuel in nitrogen.

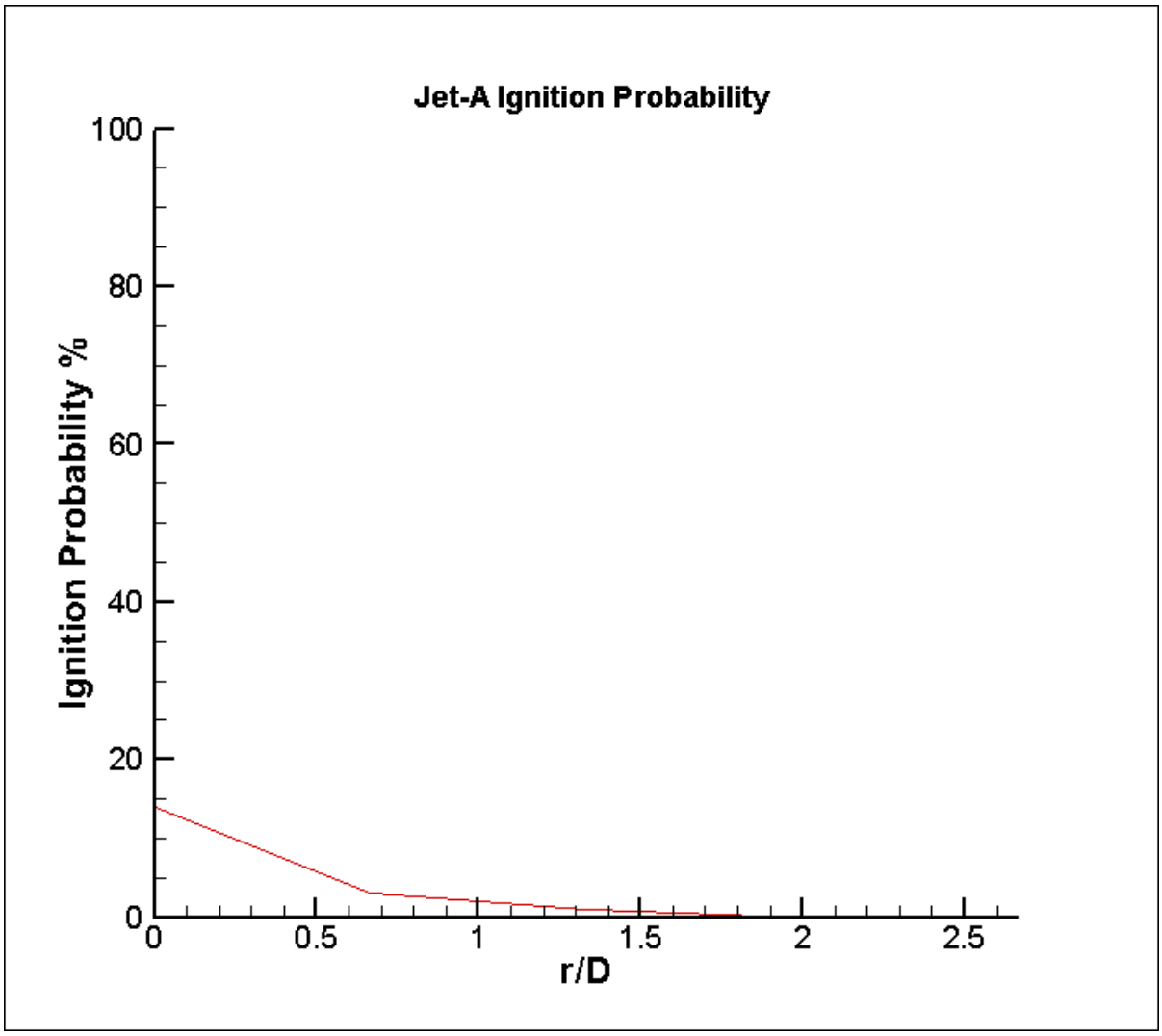

Figure 28. Ignition Probability at x/D=20 for Jet-A fuel at a 15:1 Nitrogen: Jet-A dilution ratio. The highest probability was directly above the burner at 14%.

4.4 Mean Velocity Field Measurements

The turbulent flowfield was characterized using the velocity profiles measured at a various axial locations. This was found using Particle Image Velocimetry (PIV). Velocity profiles were obtained experimentally and the results were analyzed in DaVis for both Case 1 and Case 2 (Figures 29-32). The shear layer and maximum velocity region can be clearly observed. In addition, the velocity profile at the spark inception plane was specifically studied. Figures 33-34 below show the radial profiles of the mean axial velocity at the spark inception plane

(x/D=20). It can be observed that the radial profile of the mean velocity follows the trends of a classic turbulent jet very closely [33,34]. Classical turbulent jet scaling requires an opening jet angle of 11.8°, regardless of fluid, orifice diameter, or injection speed. Case 1 for the experiment produced an opening angle of 12.1° and Case 2 produced an opening angle of 11.9°, closely matching the accepted value. Additionally, the centerline jet speed for both cases varies linearly inversely with the distance along the jet for proper turbulent mixing. The jet exit velocity was not captured in these images due to the high exit velocity of the jet relative to the air coflow. The coflow air was seeded for the PIV experiments according to best practices from previous experiments, rather than the jet tube itself.

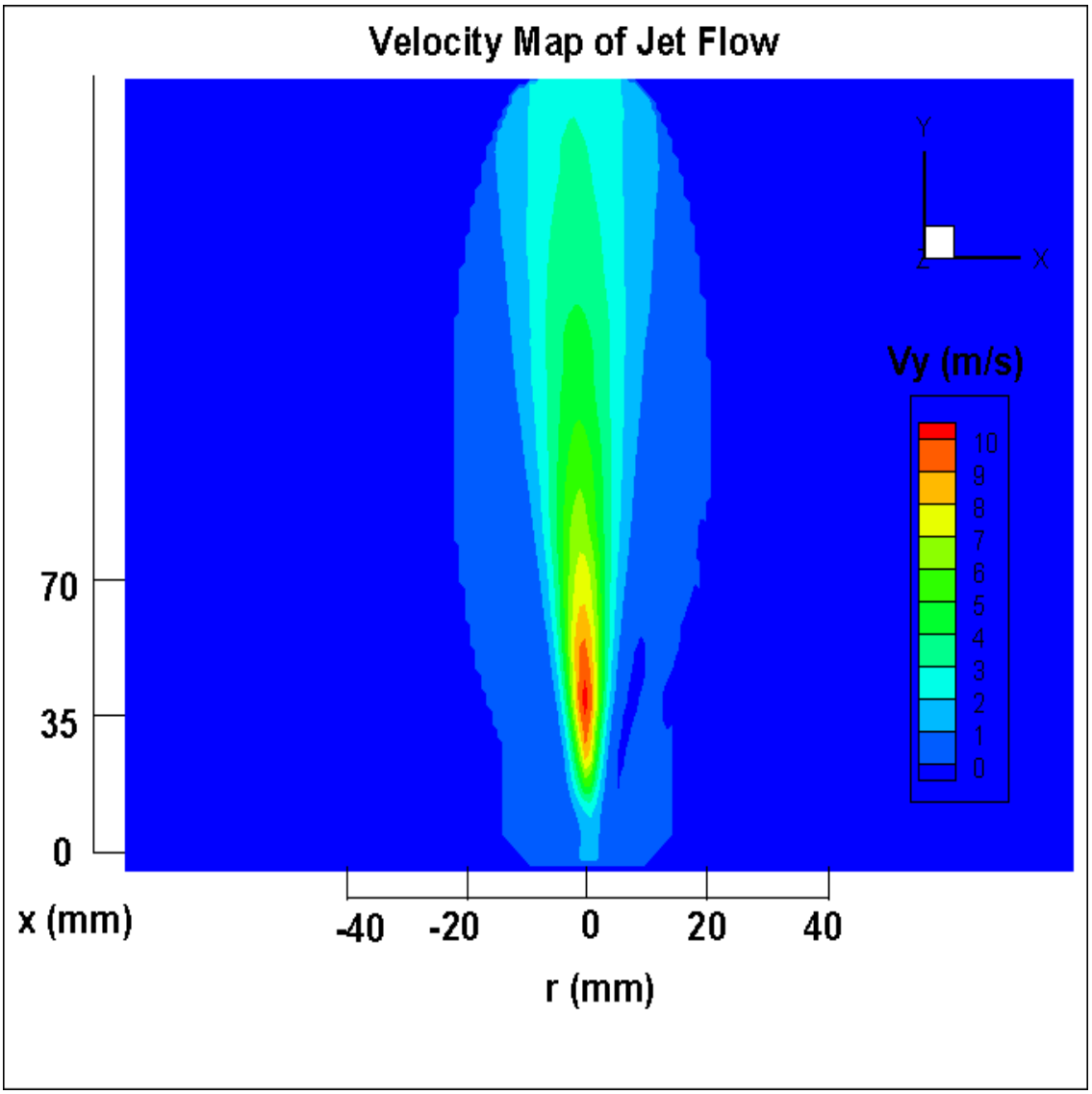

Figure 29. PIV Velocity profile from DaVis for Case 1. This provides a full map of the velocity field, with a maximum measured velocity of 10 m/s at 12 mm above the jet. The shear layer can clearly be observed at the sides of the higher velocity flowfield.

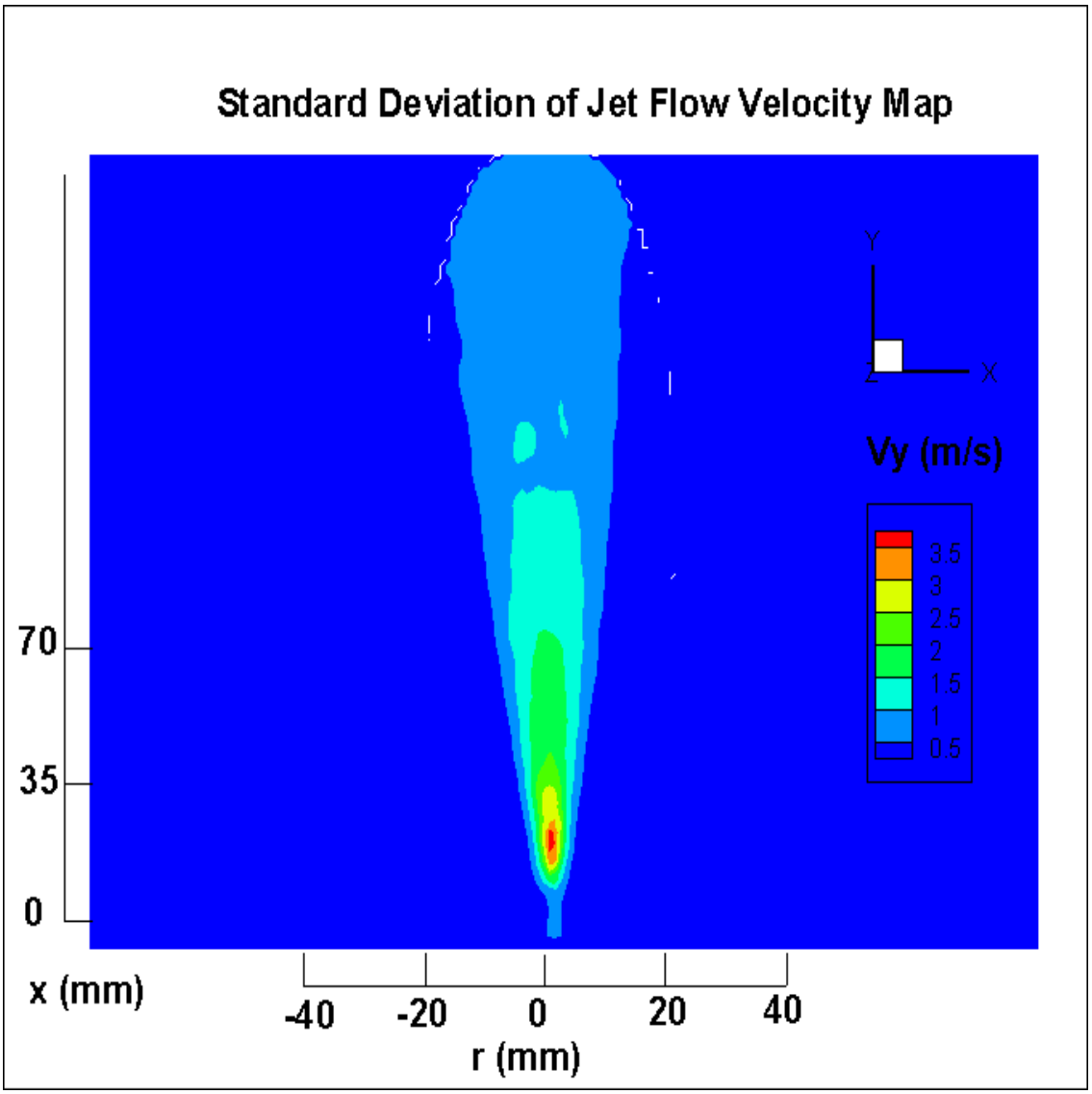

Figure 30. Standard deviation of the PIV velocity profile from DaVis for Case 1.

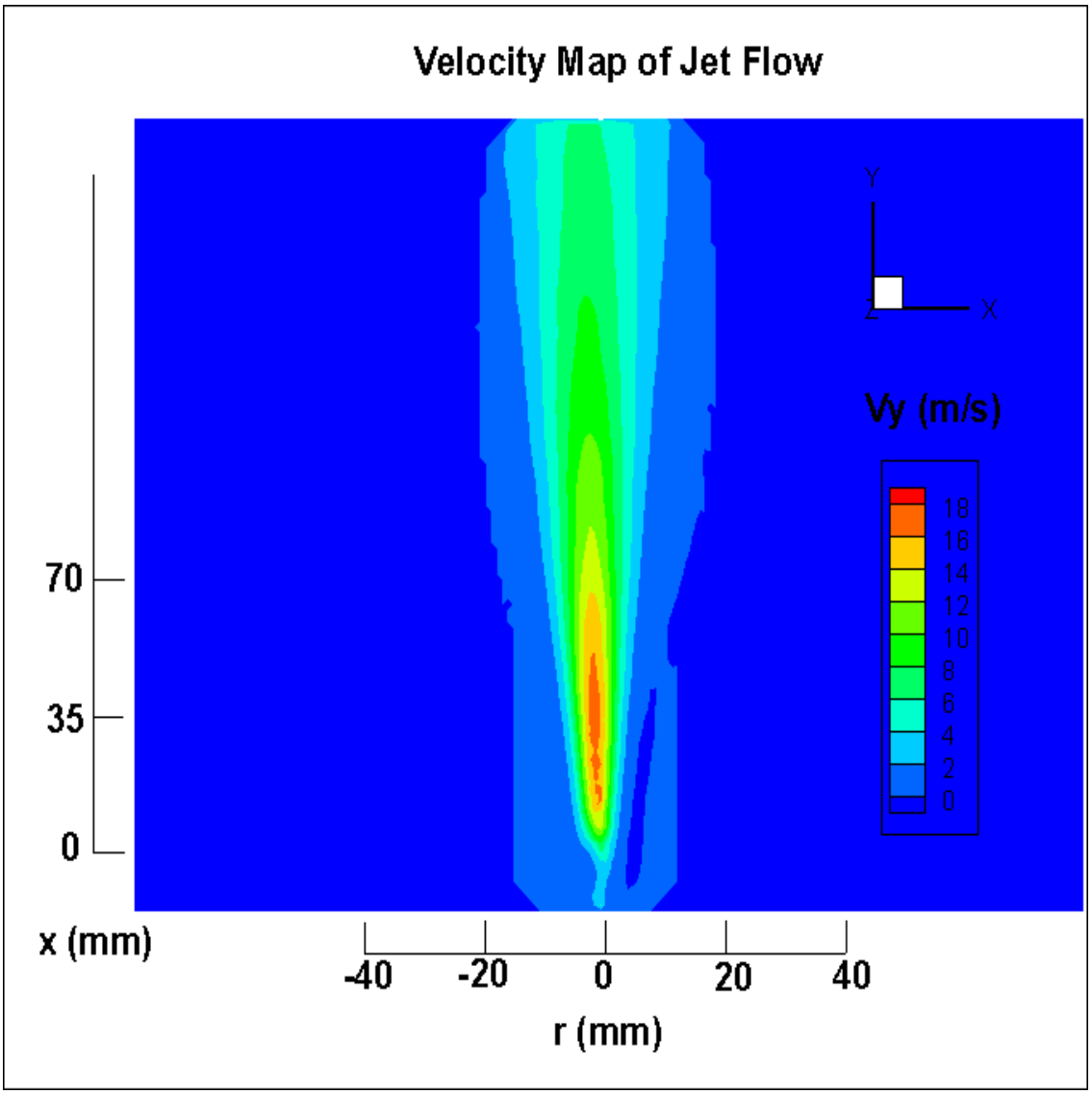

Figure 31. PIV Velocity profile from DaVis for Case 2. This provides a full map of the velocity field, with a maximum measured velocity of 18 m/s at 8 mm above the jet. The shear layer can clearly be observed at the sides of the higher velocity flowfield.

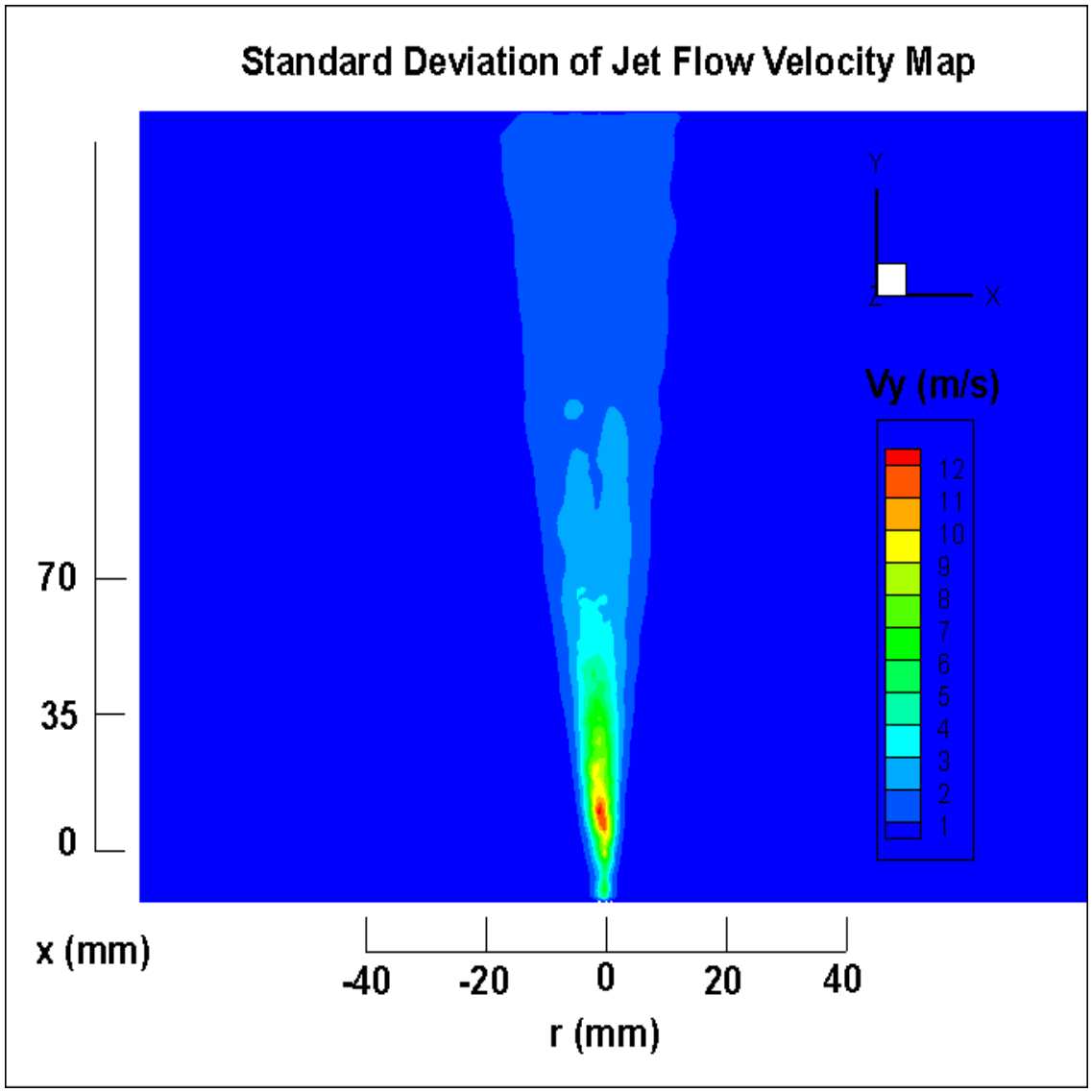

Figure 32. Standard deviation of the PIV velocity profile from DaVis for Case 2.

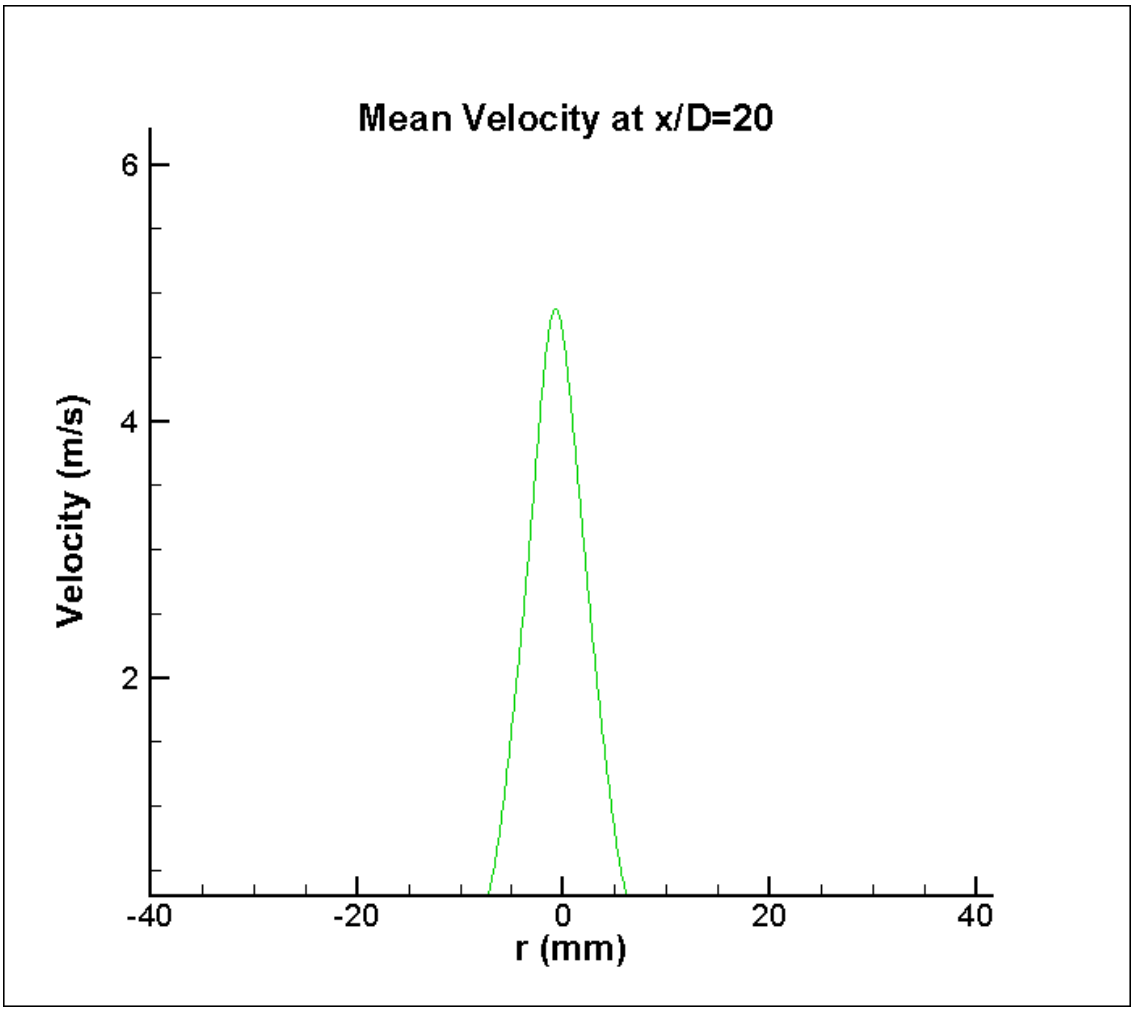

Figure 33. Mean Velocity at spark height of x/D=20 for Case 1. The max velocity was measured at 4.876 m/s.

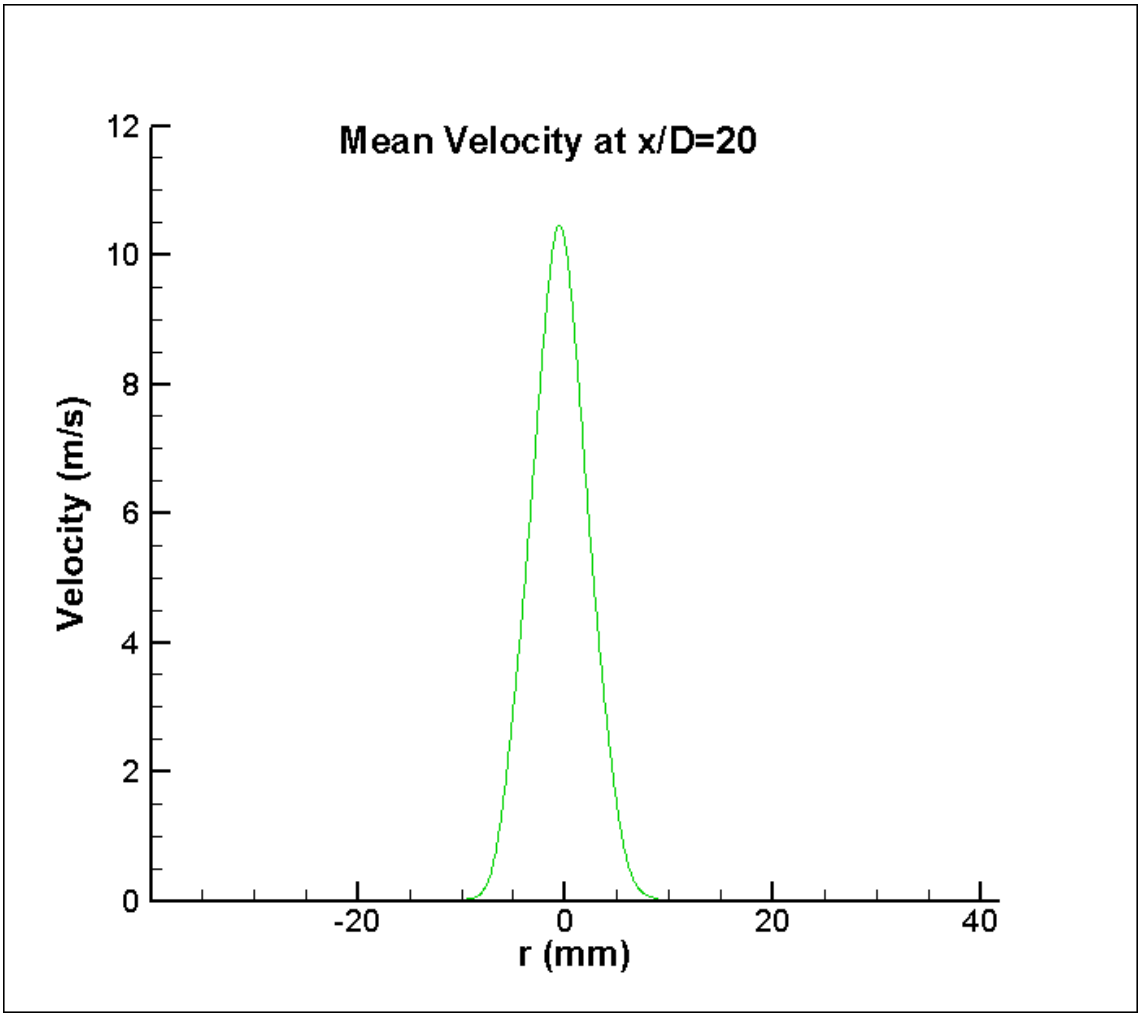

Figure 34. Mean Velocity at spark height of x/D=20 for Case 2. The max velocity was measured at 10.463 m/s.

4.5 High-Speed Imaging

High-speed images were obtained with a Photon FASTCAM CMOS camera. Initial images for finding the spark location were obtained with a 50 mm f/1.2 Nikon lens at 20,000 frames per second with a window resolution of 512x512. The trigger for the laser Q-switch was synchronized with the camera to capture the spark at the same timestamp in each video. Figure 35 and 36 below show the initial spark kernel plasma formation.

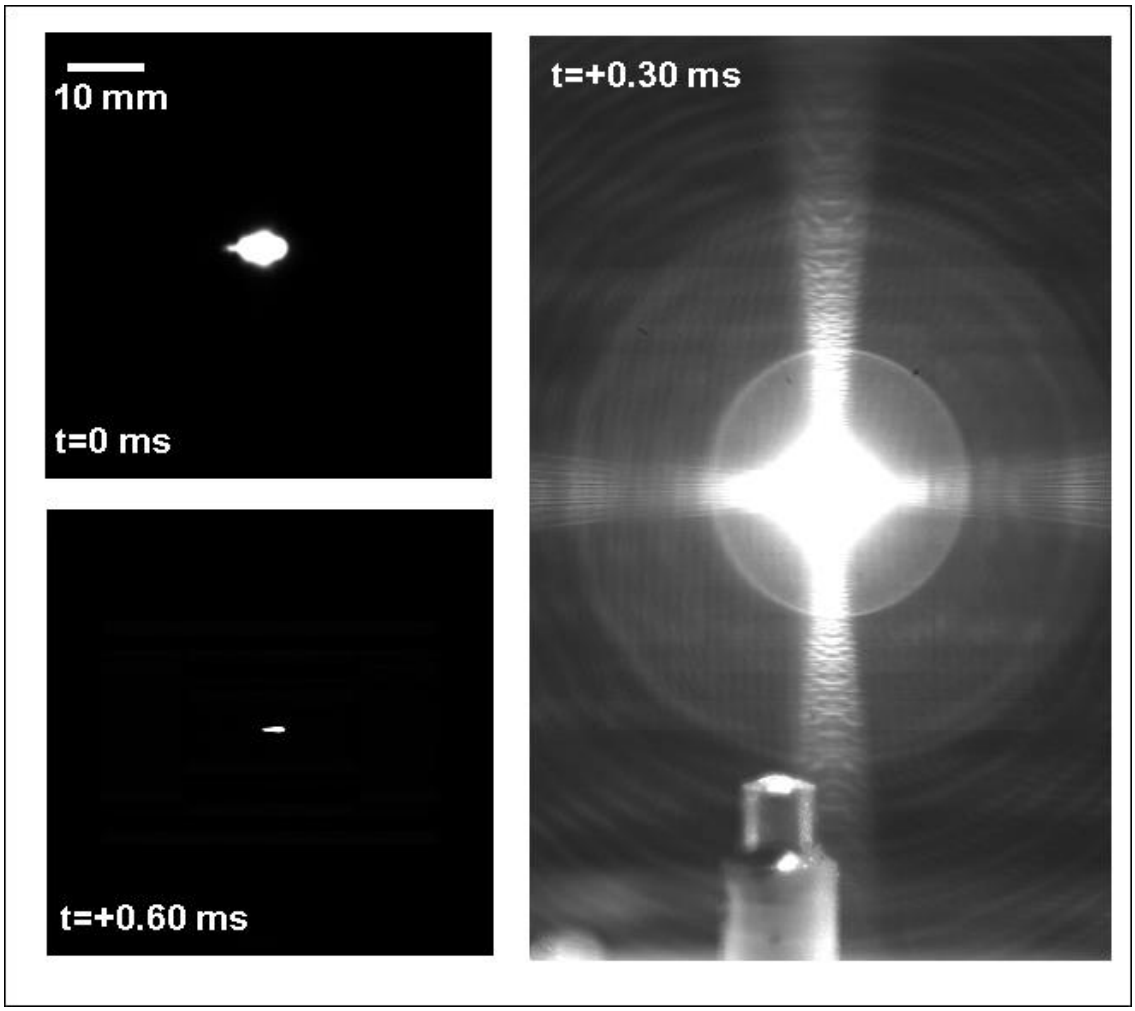

Figure 35. High-speed images of the spark kernel formation and propagation at time t=0 seconds (top left), t+0.3 ms (right), t+0.6 ms (bottom left). The tip of the jet can be seen in the right image.

4.6 Flame Luminosity

High-speed images of a successful ignition event at x/D = 40 (far above the jet tube) and r/D=0.667 (rich mixture zone) at a laser energy of 500 mJ for Case 1 parameters are shown in Figure 36. The surrounding quartz tube produced some reflections and visual artifacts in the images on the left side of each image. In the first and fourth images, the spark/flame appears as a duplicate in the reflection while the second and third images only have some minor noise artifacts. It can be observed that the initial spark kernel is circular with some fluctuations and

wrinkling around the edge, giving it a star shape. There is also some slight smearing of the spark kernel due to the presence of the fuel vapor cloud, which has a whitish fog color due to the Jet-A fuel. The subsequent images show the propagation phase as the kernel develops and interacts with the surrounding flow. It undergoes large-scale shearing as it grows in size and begins to elongate downstream due to convection before the flame was fully formed and began to propagate. Once the flame has been established, it has a noticeable tilt towards the right side of the image – away from the rich zone, into stoichiometric conditions. This aligns with the prior experiments with methane, where the successful spark kernels always propagate into the narrow composition band between the stoichiometric and lean flammability limits, away from the rich region near the center jet [32]. This was observed regardless of the spark location. This region has an ideal mixture composition to sustain the flame, as well as low aerodynamic shear to prevent reaction quenching and extinguishing of the flame.

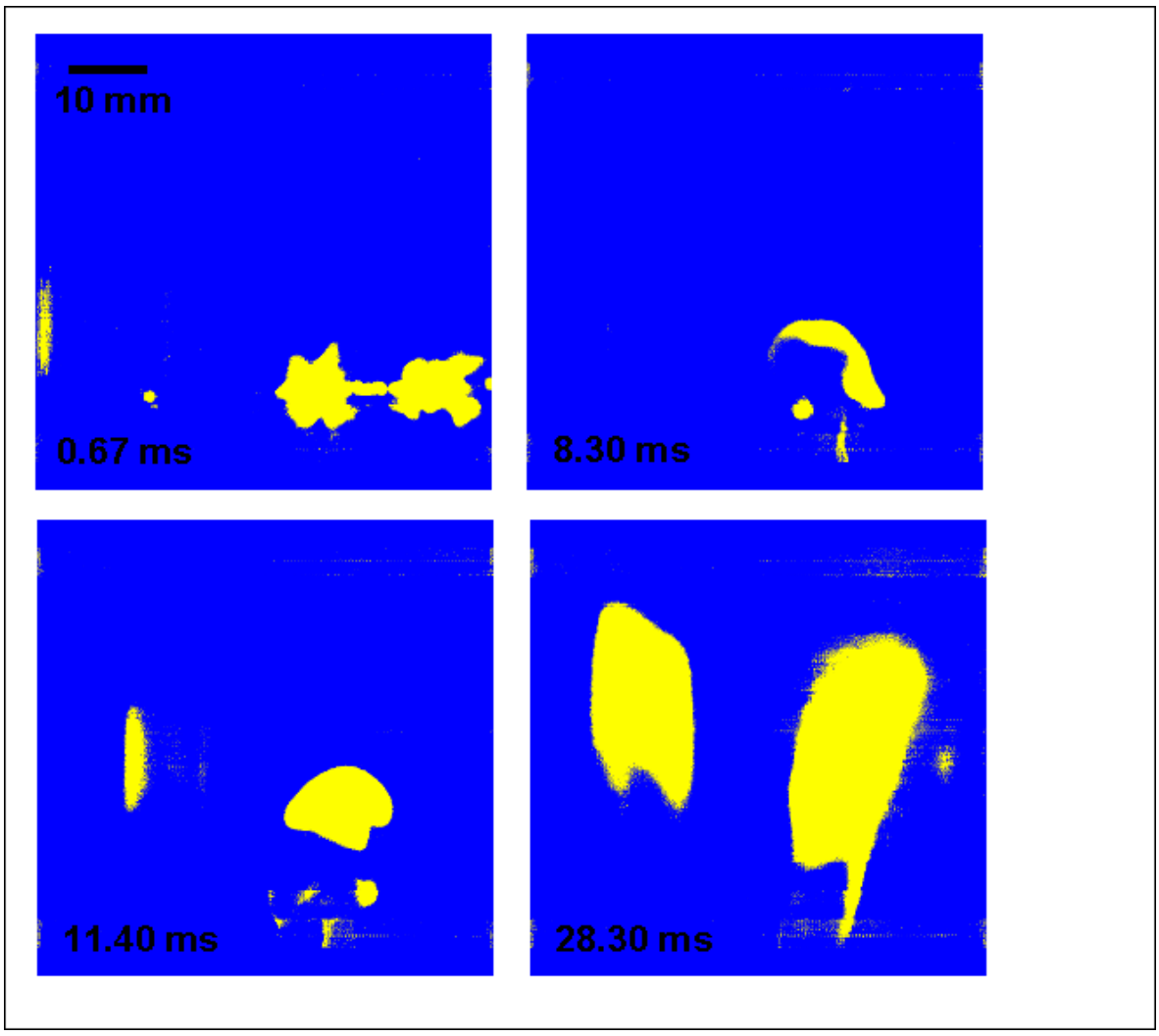

Figure 36. Flame luminosity images at x/D=40, r/D=0.667. The artifact on the left side of each image is a reflection of the spark/kernel on the quartz glass.

4.7 Chemiluminescence

High-speed images of a successful ignition event at x/D = 40 (far above the jet tube) and r/D=0.667 (rich mixture zone) at a laser energy of 500 mJ for Case 1 parameters are shown in Figure 37. For this experiment, a 420 nm filter was used to observe CH* radical formation and propagation. Chemiluminescence of CH* radicals has been demonstrated as an excellent reaction zone marker, and it has been shown previously that all the other critical radicals like OH, CN, H, etc. evolve in the same overall manner as CH* [32, 35]. Select frames of CH*

chemiluminescence from a representative ignition time sequence is presented below. It can be observed that the initial spark kernel is circular with some fluctuations and wrinkling around the edge, giving it a star shape. For these rich cases, (similar to overall flame kernel luminescence images), it can be observed that once the flame kernel pinches off from the parent plasma kernel, the reaction zones are continuously stretched by the aerodynamic shear. The reaction zones are stretched by approximately 45°, which coincides with the principal strain axis direction [32]. Alongside being stretched, the turbulent flow also transports the reaction zones outward in the radial direction, towards the right side of the image. The reaction zones in high shear, fuel rich regions are continuously quenched – there are no visible radicals in the center of the image, only towards the edges. The sustained reactions are on the zones that are transported towards the low shear, stoichiometric/lean side through flow turbulence. It is once again evident that the reactions zones at the same narrow window between the (mean) stoichiometric and lean flammability limits as observed in flame luminosity study. Regardless of where the spark is introduced, the successful kernels always tend to have the kernel base propagate into the narrow composition band between stoichiometric and lean flammability limits, where it balances low aerodynamic shear and ideal mixture composition to sustain the flame.

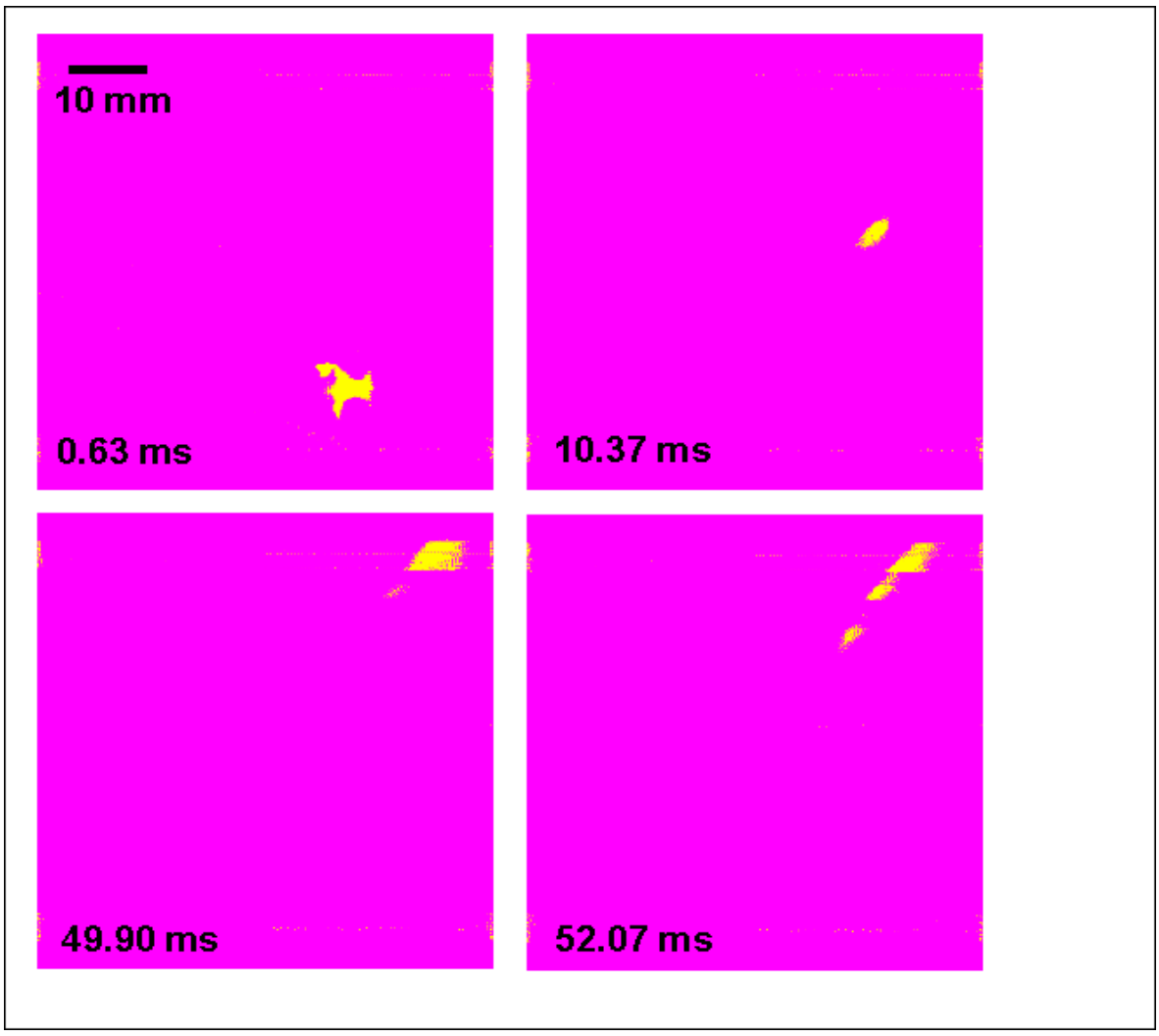

Figure 37. Chemiluminescence images at x/D=40, r/D=0.667.

4.8 Applications and Future Work

Overall, this experimental data collected provided a strong foundation for future work and left several questions for further investigation. The ignition probabilities were much lower than expected, and this may be related to the temperature profile maps. One possibility is that the fuel jet contains a small pocket of completely vaporized fuel at the center of the mixture, with fine liquid droplets surrounding it yet having the appearance of a solid vapor due to the high exit velocity and nitrogen dilution. Once a spark is deposited, the fuel vapors ignite and propagate outwards, however the plasma is not at a sufficient energy to ignite the surrounding

liquid fuel. The shear layer of the flow, being containing liquid droplets, needs a much higher energy to ignite as it must be transformed into a vapor and then into the flame kernel. The overall effect from this phenomenon is that the ignition probability is decreased due to the low temperature of the jet flow, which exists as a two-phase flow. Future work to solve this issue would involve swapping the modified JICF burner for another unit in the laboratory made from metal casings, that can handle much higher temperatures without melting. This would allow the inlet flow temperature to be significantly increased to keep the jet flow as a vapor.

Another possibility is that the jet exit velocity is so high, it is physically blowing the spark apart. Once the spark is deposited, local plasma ignites and spreads outwards. However, the jet velocity may have enough momentum to push this plasma upstream and dissipate it into the mixture, stopping the complex reactions that lead to ignition from taking place. Visual inspections during the experiments showed that flame blow-off was common, so the high exit velocity is already above the laminar flame speed. A solution for identifying this problem would be to perform additional PIV testing to obtain the laminar flame speed over all possible configurations. Then, moving the laser spark to other x/D locations and testing for ignition would give some indication of the ignition probability's spatial dependency.

5. CONCLUDING REMARKS

Efforts to develop a spark ignition system for Jet-A fuel at several axial spark locations were discussed, and the best-practices for experimental safety, results of ignition probability maps, and high-speed imaging of the plasma kernel were presented. Future experiments will seek to identify the source of low ignition rates with higher temperature flow and parametric analysis of the spark location.

6. REFERENCES

1. Ahmed, S.F., and E. Mastorakos. “Spark Ignition of Turbulent Spray Flames”. Combustion Institute, 2006.
2. Spark Plug Image. Matthew’s Volvo Site. https://www.matthewsvolvosite.com/
3. Spark Plug Image. “No Spark Guide for Negative Earth Distributors. https://blog.simonbbc.com/
4. Combustion Image. GarageSpot. https://garagespot.com/
5. Marchione, T., S.F. Ahmed, E. Mastorakos. “Ignition of Turbulent Spray Flames Using Single and Multiple Sparks”. Combustion and Flame. 2009.
6. Flame Image. Bureau of Fire Safety. http://www.hopewelltwp.org/252/Bureau-of-Fire-Safety
7. Ahmed, Samer Fikry Abdel Fattah Sayed. “Spark Ignition of Turbulent Spray Flames”. Ph.D Dissertation, 2006.
8. Military Heavy Fuel Images. Army Webpage. http://www.alu.army.mil/
9. Laminar to Turbulent Transition Image. http://keywordsuggest.org/gallery/856898.html
10. Sforzo, Brandon. “High Energy Spark Ignition in Non-Premixed Flowing Conbustors”. Ph.D Dissertation, 2014.
11. Mastorakos, E. “Forced Ignition of Turbulent Spray Flames”. Combustion Institute. 2017.
12. Ballal, D. R., and A.H. Lefebre. “A General Model of Spark Ignition for Gaseous and Liquid Fuel Mixtures”. Combustion Institute, 1981.
13. Ballal, D. R., and A.H. Lefebre. “Ignition of Liquid Fuel Sprays at Subatomic Pressures”. Combusiton and Flame 31, 115-126, 1978.
14. Ballal, D. R., and A.H. Lefebre. “Ignition and Flame Quenching of Flowing Heterogeneous Fuel-Air Mixtures”. Combustion and Flame 35, 155-168, 1979.
15. Cochet, M. et al. “Evaporation of Polydispersed Droplets in a Highly Turbulent Channel Flow”. Exp Fluids 47, 379-394, 2009.

16. Shelby, Michael H., Brad A VanDerWege, and Simone Hochgreb. “Early Spray Developments in Gasoline Direct-Injected Spark Ignition Engines”. International Congress and Exposition, 1998.
17. O’Loughlin, William, and Assaad R. Masri. “The Structure of Auto-Ignition Region in Turbulent Dilute Methanal Sprays Issuing in a Vitiated Co-flow”. Flow Turbulence Combustion 89, 13-35, 2012.
18. Kourmatzis, A., W. O’Loughlin, and A. R. Masri. “Effects of Turbulence, Eveporation, and Heat Release on the Dispersion of Droplets in Dilute Spray Jets and Flames”. Flow Turbulence Combustion 91, 405-427, 2013.
19. Lyons, O. F. P., T. Persoons, and D.B. Murray. “Particle Sizing and Flow Measurements in an Atomizing Mist Jet Nozzle: A Shadowgraphy Approach”. ILASS 2010.
20. Romero, D, N. Parthasarathy, S. R. Gollahalli. “Laminar Flame Characteristics of Partially Premixed Prevaporized Palm Methyl Ester and Diesel Flames”. Journal of Energy Resources Technology 136, 2014.
21. Dhanuka, Sulabh K., Jacob E. Temme, and James F. Driscoll. “Unsteady Aspects of Lean Premixed Prevaporized Gas Turbine Combustors: Flame-Flame Interactions”. Propulsion and Power Vol. 27 No. 3, 2011.
22. Aida, Naoki, et al. “Combustion of Lean Prevaporized Fuel-Air Mixtures Mixed with Hot Burned Gas for Low-NOX Emissions Over An Extended Range of Fuel-Air Ratios”. Combustion Institute 2005.
23. Beck, C. H., R. Koch, H.-J. Bauer. “Identification of Droplet Burning Modes in Lean, Partially Premixed Swirl-Stabilized Spray Flames.” Combustion Institute 2009.
24. Dhanuka, Sulabh K.,et al. “Vortex-Shedding and Mixing Layer Effects on Periodic Flashback in a Lean Premixed Prevaporized Gas Turbine Combustor”. Combustion Institute 2009.
25. Love, N. D., R. N. Parthasarathy, S. R. Gollahalli. “Rapid Characterization of Radiation and Pollutant Emissions of Biodiesel and Hydrocarbon Liquid Fuels”. Journal of Energy Resources Technology 2009.

26. Gokulakrishnan, P., et al. “A Novel Low NOX, Lean, Premixed, and Prevaporized Combustion System for Liquid Fuels”. Journal of Engineering for Gas Turbines and Power, 2008.
27. Roby, Richard J, et al. “Development of a System for Lean, Prevaporized, Premixed Combustion”. Proceedings of the Thirty-Sixth Turbomachinery Symposium, 2007.
28. Allouis, C., F. Beretta, and A. Amoresano. “Experimental Study of Lean Premixed Prevaporized Combustion Fluctuations in a Gas Turbine Burner”. Combustion Science and Technology, 2008.
29. Holley, A. T., et al. “Extinction of Premixed Flames of Practical Liquid Fuels: Experiments and Simulations”. Combustion and Flame 144, 448-460, 2008.
30. El-Rabii, H., et al. “Laser Ignition in a Lean Premixed Prevaporized Injector”. Combustion Science and Technology 2010.
31. Shehata, Mohamed S., Mohamed M. ElKotb, and Hindawi Salem. “Combustion Characteristics for Turbulent Prevaporized Premixed Flame Using Commerical Light Diesel and Kerosene Fuels”. Journal of Combustion 2014.
32. Ley, K. and Narayanaswamy, V. “Parametric Study of Forced Ignition in Laminar and Turbulent Methane Jets”. 2017.
33. Gampert, Markus, Venkat Narayanaswamy, Norbert Peters. “Scalar Gradient Trajectory Measurements Using High-Frequency Cinematographic Planar Rayleigh Scattering”. Exp Fluids 54, 2621, 2013.
34. Cushman-Roisin, Benoit. “Turbulent Jets.” Thayer School of Engineering, Dartmouth College. 2017.
35. Chen, L.D., et al., Buoyant diffusion flames. Symposium (International) on Combustion, 1989. 22(1): p. 677-684.